Tellus
SERIES B
CHEMICAL
AND PHYSICAL
METEOROLOGY
PUBLISHED BY THE INTERNATIONAL METEOROLOGICAL INSTITUTE IN STOCKHOLM

Tellus (2008), 60B, 604–621

TELLUS

Environmental controls on the stable carbon isotopic composition of soil organic carbon: implications for modelling the distribution of C_3 and C_4 plants, Australia

By JONATHAN G. WYNN[1]* and MICHAEL I. BIRD[2], [1]*Department of Geology, University of South Florida, Tampa, FL 33620, USA;* [2]*School of Geography and Geosciences, University of St. Andrews, St. Andrews, Fife, KY16 9AL, Scotland, UK*

(Manuscript received 25 July 2007; in final form 21 April 2008)

ABSTRACT

We use multivariate statistics to examine the continental-scale patterns of the stable carbon isotopic composition ($\delta^{13}C$) of soil organic carbon (SOC) from a data set collected throughout the natural range of variation in climatic, edaphic and biotic controls in Australia. Climate and soil texture (percent of mineral particles <63 μm) are found to be the dominant controls on $\delta^{13}C_{SOC}$. Of the environmental variables analysed, the strongest correlations to $\delta^{13}C_{SOC}$ do not simply occur with respect to mean annual temperature or precipitation, but rather to ecosystem-scale measures of water availability such as mean annual vapour pressure deficit (VPD) and an index of the annual flux of available water available to plants (W). After the variance of $\delta^{13}C_{SOC}$ attributed to W was removed, the proportion of particles ≤ 63 μm diameter remained the only secondarily significant correlation ($p < 0.05$). Based on this observation, we also develop a model of the primary climatic control on $\delta^{13}C_{SOC}$, which is rooted in the assumption of optimized water-use efficiency of C_3 and C_4 vegetation, and can be extrapolated to continental or global data with readily available environmental data. The model describes optimized water-use efficiency controls on $\delta^{13}C_{SOC}$ in terms of a function of the variable W. We estimate model parameters of climatic control on $\delta^{13}C_{SOC}$ using an analysis of surface samples (0–5 cm) of sandy soils ($<10\%$ mineral particles ≤ 63 μm diameter) from which other edaphic and biotic controls are minimized. This simple model function is modified to account for variation of $\delta^{13}C_{SOC}$ due to variation of respiration rates and variable incorporation of the terrestrial Suess effect with mean annual temperature (MAT). Model regression of $\delta^{13}C_{SOC}$ to these continental-scale climate data accounts for 92% of the variance observed using a model function with simple variables (W and MAT) and physically meaningful constants. We also examine edaphic controls on $\delta^{13}C_{SOC}$ using particle size separates from soil textural gradients within four climatic zones of Australia. These data indicate the protection of ^{13}C-enriched old, stable SOC in association with fine mineral particles, consistent with variable incorporation of the terrestrial Suess effect.

1. Introduction

Accurate model predictions of the global carbon (C) cycle depend heavily on estimates of global patterns of the stable C isotopic composition ($\delta^{13}C$) of the terrestrial biosphere and C fluxes between biosphere and atmosphere. Natural abundance stable isotope studies provide one of the most effective means of constraining uncertain components of the global carbon (C) cycle, such as the net carbon exchange between the terrestrial biosphere and atmospheric reservoirs, and the size and partitioning of terrestrial carbon reservoirs (Flanagan et al., 2005). These stable isotope model estimates are crucial to understanding temporal and spatial variation in atmospheric CO_2 sources and sinks, and partitioning fluxes into terrestrial and marine components (Keeling et al., 1989; Ciais et al., 1995; Francey et al., 1995; Battle et al., 2000). One critical parameter in global C cycle models is the fractional contribution of C_4 plants to terrestrial primary productivity, because the $^{13}CO_2$ discrimination by C_4 plants is similar to the effect observed for air–sea CO_2 exchange, and highly dissimilar to that of their C_3 counterpart (Ciais et al., 1995; Fung et al., 1997; Suits et al., 2005).

Global estimates of the $^{13}CO_2$ discrimination by the terrestrial biosphere are based on modelling of ecophysiological processes at the leaf and plant scale and scaling these observations up to

*Corresponding author.
e-mail: jwynn@cas.usf.edu
DOI: 10.1111/j.1600-0889.2008.00361.x

the regional or global scale (Lloyd and Farquhar, 1994; Still et al., 2003). Meanwhile, attempts to measure regional to global average $\delta^{13}C$ of the terrestrial biosphere are hindered by analytical and scaling considerations (Bird et al., 2001). One potential method of empirical validation of global models of C_4 photosynthesis is by quantification of the spatial patterns of the $\delta^{13}C$ value of soil organic carbon (SOC) as a measure of the proportional contribution of each of the two dominant photosynthetic pathways to a C reservoir with a longer mean residence time than biomass, and thus greater temporal averaging (Bird and Pousai, 1997). Despite this potential, global representation of stable isotopic processes occurring in the SOC pool of the terrestrial biosphere remains one of the most uncertain components of terrestrial C exchange models (Randerson et al., 2002; Ciais et al., 2005), in part due to a lack of data collected systematically using standardized field and laboratory protocols over broad climatic regions (Bird et al., 2001).

Our recent work (Wynn et al., 2006) examined variation in SOC inventory at the scale of the Australian continent, but also presented stable carbon isotope data ($\delta^{13}C_{SOC}$) in an accompanying online supplement, as part of a longer-term effort to establish data sets collected along regional environmental gradients using standardized protocols (Bird and Pousai, 1997; Bird et al., 2002a, b, 2003). In this paper, we (1) use statistical tests to examine the relative roles of environmental controls on $\delta^{13}C_{SOC}$ in this data set and (2) model these environmental controls with parameters defined by model-data fusion. The output of this study is a mechanistic model of the environmental control on the distribution of C_3 and C_4 biomass that is based on the fundamental control of the annual amount of water available to an ecosystem for plant physiological processes and the differences in efficiency with which mixed C_3–C_4 ecosystems use the available water.

1.1. A review of environmental controls on the carbon isotopic composition of terrestrial biomass and soil organic carbon

The wide range of $^{13}C/^{12}C$ ratios in plants derives primarily from markedly different ^{13}C-discrimination during photosynthesis following one of three pathways (C_3, C_4 and CAM; Farquhar et al., 1980; Hatch, 1987; Nobel, 1994; Sage, 2004). $\delta^{13}C$ values of living plant biomass ($\delta^{13}C_p$), and of the fluxes between terrestrial biomass and atmosphere CO_2 are primarily controlled by distribution of plants assimilating C via these three photosynthetic pathways. Spatial variability of C_3 and C_4 plants occurs at a variety of scales, and follows macro- and microclimatic, as well as edaphic variables all of which control the growth and survival of plants that utilize each pathway (Teeri, 1988). The distribution of C_3 and C_4 plants is most fundamentally controlled by differences in their success at competing for resources necessary for physiological processes such as photosynthesis, respiration and transpiration. Rates of primary productivity depend on rates of utilization of the primary resources, which include solar energy, CO_2, H_2O, O_2, as well as nitrogen (N) and other nutrients. Thus the fundamental controls on C_3 and C_4 distribution reduce to the availability of these primary resources in the environment, the efficiency with which plants can take up these resources under variable environmental conditions, and kinetic controls on physiological reaction rates, which are controlled by temperature at the reaction sites (leaf temperature). These effects can be framed in terms of a model of quantum yield for CO_2 fixation which describes the rate of net CO_2 fixation per unit photosynthetically active radiation (PAR) under variable resource availability (Ehleringer and Björkman, 1977). This, and many studies since, have concluded that the competitive advantage of C_4 plants is maximized independently under the conditions of high availability of light, high availability of O_2, low availability of CO_2, low availability of H_2O, low availability of N, and high leaf temperatures (O'Leary, 1981; Ehleringer et al., 1986, 1997; Sage and Pearcy, 1987; Farquhar et al., 1988; Teeri, 1988; Buchmann et al., 1996; Collatz et al., 1998). Each of these controls can be quantified independently under controlled environmental conditions, but the combined effects of several influences operating at the scale of ecosystems is much more complex. In general, the environmental constraints on C_3 and C_4 plant distribution at the scale of ecosystems or biomes have been framed in terms of a model of CO_2 crossover leaf temperature. Above the crossover leaf temperature, C_4 plants are more competitive at photosynthesis due to the increased rate of photorespiration in C_3 plants at higher leaf temperatures (Ehleringer and Björkman, 1977; Collatz et al., 1998). The crossover leaf temperature model emphasizes the fundamental importance of atmospheric p_{CO_2} and leaf temperature, and remains the most commonly used model for understanding variations in C_3 and C_4 primary productivity (Ehleringer et al., 1997; Collatz et al., 1998; Still et al., 2003; Suits et al., 2005). Many empirical studies of the distribution of C_3 and C_4 plants have extended this construct to very high statistical correlations between the fractional contribution of C_4 plants and various expressions of environmental temperature (normal summer minimum temperature, mean annual degree days, summer average temperature, growing season temperature, etc.). It is also widely recognized that these climatic variables are only proxies for the kinetic effects of leaf temperature effects described above (Teeri, 1988).

Within these environmental constraints, $\delta^{13}C_p$ of C_3 plants varies from about -34 to -20‰ (*cf.* Deines, 1980). This within-pathway variation is primarily attributed to environmental controls of drought stress (i.e. water availability) and irradiance, both of which act through control of the ratio of internal to atmospheric CO_2 concentration (p_i/p_a; Ehleringer et al., 1986, 1993; Farquhar et al., 1989). Drought stress simultaneously reduces photosynthesis and transpiration rates by reducing stomatal conductance. Drought-induced increases in leaf-to-air vapour pressure deficit (VPD) result in decreased p_{CO_2} inside leaves (p_i) and thus decreased discrimination (Δ_{B-C_3}) and ^{13}C-enriched $\delta^{13}C_p$ values (Farquhar et al., 1982a; Winter et al., 1982;

Farquhar and Richards, 1984; Brugnoli et al., 1988). Although studies of within-canopy irradiance levels show that as irradiance is reduced p_i increases and $\delta^{13}C_p$ of leaves decreases (lower in the canopy; Ehleringer et al., 1986), these effects are difficult to distinguish from those of drought stress in field conditions (Farquhar et al., 1989).

Additional environmental controls on $\delta^{13}C_p$ of C_3 plants include the 'canopy effect,' (Vogel, 1978; van der Merwe and Medina, 1989) and differences between plant functional groups (for example evergreen plants are more ^{13}C-enriched by $\sim$1‰; Stuiver and Braziunas, 1987; DeLucia and Schlesinger, 1991; Marshall and Zhang, 1994).

Within the C_4 photosynthetic pathway, $\delta^{13}C_p$ varies much less than within the C_3 group (-9 to -16‰), and the variation can be primarily attributed to availability of water and light (Ehleringer, 1993; Buchmann et al., 1996). Edaphic factors such as salinity stress, in turn control the effective availability of water (Sandquist and Ehleringer, 1995).

In order to use $\delta^{13}C$ of SOC to interpret global patterns of C_3 and C_4 photosynthesis, we must also consider key carbon isotopic effects occurring during C cycling through the SOC pool. These include kinetic fractionation against ^{13}C during SOM decomposition, combined with the stabilization of the ^{13}C-enriched solid decomposition products, which is enhanced by interaction with fine mineral particles (Ågren et al., 1996; Šantrůčková et al., 2000; Wynn et al., 2005), the 'terrestrial Suess effect (Bird et al., 1996), and selective preservation of components of biomass, such as relatively stable lignin-derived compounds (Boutton, 1996; Schleser et al., 1999).

2. Methods

2.1. Soil sampling and analytical methods

To account for variability of $\delta^{13}C_{SOC}$ at the local and regional scale (on the order of 10–100 km^2), and in order to extend these regional scale measurements to the continental scale, we utilized a stratified sampling approach that divides the landscape into sampling locations locally dominated by C_3 or C_4 vegetation in mixed C_3–C_4 ecosystems ('tree' and 'grass' samples, for details of methodology see Wynn et al., 2006). Regions were selected for minimal anthropogenic disturbance (no agriculture), although many have been grazed by both native species and livestock. Analyses of the 'tree' and 'grass' samples are then apportioned according to the estimates of the fractional canopy cover of the region to provide a weighted SOC inventory and ecosystem-scale $\delta^{13}C_{SOC}$ estimate. Fractional canopy cover was estimated on an aerial basis at each of the 25 sampling sites within each region. For regions with greater than 50% canopy cover, the 'tree' and 'grass' samples were apportioned equally for the entire site.

At each of 48 ecosystem regions of Australia (Fig. 1), a total of 200 soil cores were collected according to the protocol outlined in detail by Wynn et al. (2006) to produce four bulked samples representative of each region (0–5 cm tree, 0–5 cm grass, 0–30 cm tree and 0–30 cm grass). Variance of $\delta^{13}C_{SOC}$ is estimated by a set of 20 samples from each region, bulked along five transects for each of the four sample types described above. For this study, $\delta^{13}C_{SOC}$ values were calculated separately for the 0–5 cm and 5–30 cm depth intervals using a mass balance approach based on measurements of the 0–5 and 0–30 cm samples. C concentration and $\delta^{13}C$ of CO_2 produced by combustion of SOC was measured by a combination of dual-inlet mass spectrometry and elemental analysis-continuous flow mass spectrometry at the Research School of Earth Sciences, Australian National University, and the School of Geography and Geosciences at the University of St. Andrews. SOC data used in this modelling study are reported in the database accompanying Wynn et al. (2006).

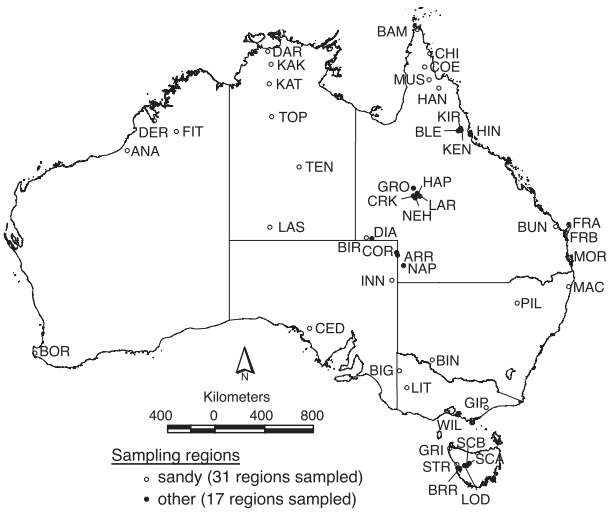

Fig. 1. Location map of sites sampled in this study.

2.2. Environmental variables and statistical analyses

SPSS version 14.0 was employed for factor analysis and linear regression analysis using environmental variables and $\delta^{13}C_{SOC}$ measurements. Factor analysis was performed on the correlation matrix derived from the following environmental variables: fraction of woody biomass cover (f_w), mean annual temperature (MAT, K), mean annual precipitation (MAP rate, mol H_2O m^{-2} yr^{-1}), 1/VPD (kPa^{-1}; VPD, mean annual vapour pressure deficit, inverted to be consistent in sense with positive moisture availability), annual water availability (W, mol H_2O m^{-2} yr^{-1}), mean annual normalized difference vegetation Index (ndvi, values from -1 to 1 linearly scaled up to integers from 0 to 255), $f_{<63\,\mu m}$ (fraction of soil solids <63 μm diameter), pH (acidity), SOC (SOC inventory, mol C m^{-2}) and N (soil nitrogen inventory, mol N m^{-2}). The component transformation matrix and plot are shown (Fig. 2) in rotated space

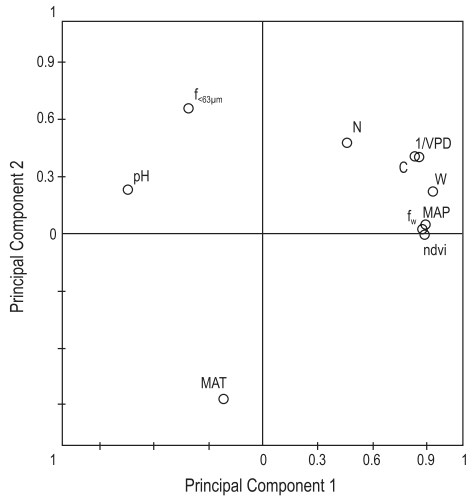

Fig. 2. Principal component analysis plot in rotated space for environmental variables potentially controlling $\delta^{13}C_{SOC}$.

(rotated according to the varimax method). Also, stepwise linear regression was performed on the following variables: f_w, MAT, MAP, W, 1/VPD, ndvi, $f_{<63\,\mu m}$, pH, SOC, N and the SOC:N ratio (a measure of litter quality).

Our employed measure of the annual flux of water available to plants (W) takes into account mean annual precipitation flux and evaporative flux calculated assuming all global solar radiation flux at the soil surface went into evapotranspiration (based on Berry and Roderick, 2002a):

$$W = \mathrm{MAP} - Q_s/\rho_w L, \tag{1}$$

where MAP is mean annual precipitation rate in kmol H_2O m^{-2} yr^{-1}, Q_s is mean annual all-wave global solar radiation flux in kJ m^{-2} yr^{-1}, ρ_w is the density of liquid water (~55.5 kmol m^{-3} at 298.15 K) and L is the latent heat of evaporation of water (~45 kJ mol^{-1} H_2O at 298.15 K). Water fluxes (MAP, Q_s/ρ_w L and W) are most commonly conceived in dimensions of length/time (such as m H_2O yr^{-1}), but can also be reduced to (kmol H_2O m^{-2} yr^{-1}) by multiplying by the density of liquid water and converting kg to kmol.

2.3. *Development of an optimized water use efficiency model applied to SOC*

We derive a model equation describing the $\delta^{13}C$ value of C assimilated into the SOC pool which is based on the fundamental assumptions of the well-established optimized stomatal behaviour model (Cowan, 1977; Cowan and Farquhar, 1977), also used as the basis for a model of ^{13}C discrimination by the terrestrial biosphere (Δ_B; Lloyd and Farquhar, 1994). Our model of SOC is founded on the assumption that ecophysiological differences between and within the C_3 and C_4 photosynthetic pathways result in differences in their relative contribution to SOC storage. The model calculates mixing of $\delta^{13}C_{SOC}$ from the proportions of SOC derived from C_3 and C_4 plants and estimates of the $\delta^{13}C_{SOC}$ values of C_3 and C_4 plants.

2.3.1. Background. The Cowan–Farquhar model is rooted in the assumption that stomata are optimized to maximize plant C assimilation (A; mol CO_2 m^{-2} s^{-1}) with respect to plant water loss (E; mol H_2O m^{-2} s^{-1}), and thus the marginal cost (in H_2O) of assimilating CO_2 is constant during the day ($\partial E/\partial A = \lambda = \text{const.}$). The Lloyd–Farquhar model makes an extension of Cowan–Farquhar equation to stomatal control of Δ_B, and extends these theoretically based relationships with global gross primary productivity (GPP) to calculate global patterns of Δ_B and the global distribution of C_4 photosynthesis. Thus, in the Lloyd–Farquhar model, a primary environmental control on spatial patterns in Δ_B is the leaf-to-air vapour mole fraction difference (D, mmol mol^{-1}), which is directly related to E. Our model extends the Cowan–Farquhar and Lloyd–Farquhar relationships to SOC assuming (1) assimilation is from a constant $\delta^{13}C_{CO_2}$, and thus there is a 1:1 relationship between $\delta^{13}C_p$ and Δ_B (i.e. minimal canopy effect of Vogel, 1978) and (2) that no isotopic effects occur in biomass C-SOC flux in the sandy, well-drained soils measured (i.e. a similar 1:1 relationship between $\delta^{13}C_p$ and, and $\delta^{13}C_{SOC}$ holds, see discussion below), and (3) that the environmental control of E on Δ_B, (and thus on $\delta^{13}C_p$ and $\delta^{13}C_{SOC}$) is accounted for by our index of the annual availability of water, W. Our model is thus based entirely on optimized water-use efficiency.

C_4 plants have a competitive advantage over their C_3 counterparts under H_2O- and CO_2-limited conditions, given their high water use efficiency of photosynthesis (WUE_{ph}; Osmond et al., 1982; Ehleringer et al., 1991). The higher WUE_{ph} of C_4 plants is observable from stomatal gas exchange measurements (Schulze and Hall, 1982), as well as canopy scale measurements of CO_2 and H_2O vapour exchange over C_3 and C_4 vegetation (Grace et al., 1998; Long, 1999). The higher WUE_{ph} of C_4 plants is controlled primarily by stomatal conductance, because CO_2 assimilation and H_2O vapour loss share the same diffusion pathway through stomata. Because stomatal conductance is also the primary physiological control on diffusional discrimination against ^{13}C, WUE_{ph} is well reflected in differences of $\delta^{13}C_p$ values between C_3 and C_4 pathways, and within the C_3 pathway (Farquhar et al., 1988, 1989; Comstock and Ehleringer, 1992; Ehleringer, 1993; Brugnoli and Farquhar, 2000; Sage, 2004). The water use advantage of C_4 versus C_3 plants provides the critical linkage between plant ecophysiology and SOC isotope ratios as the basis of our model.

2.3.1.2. Water availability versus leaf temperature as the climatic control of C_3–C_4 distribution. Our mechanistic model simplifies climatic control on the distribution of C_3 and C_4 plants relying on the assumptions that water is the limiting factor in

C_3 versus C_4 photosynthesis, and that water-limited ecosystems tend to optimize WUE_{ph} within the boundaries of plant physiological constraints. This approach thus differs from the dominantly temperature-based model C_3–C_4 distributions produced by Still et al. (2003). It is well known that leaf temperature is a direct control on net photosynthesis rates of C_3 and C_4 plants (Ehleringer and Björkman, 1977) through kinetic control on gross photosynthesis and photorespiration rates (Nobel, 2005). As leaf temperature is increased in C_3 plants, the rate of photorespiration increases faster than the rate of photosynthesis. Consequently at higher leaf temperatures, C_3 plants must expend more energy per unit net CO_2 assimilation because an increasing proportion of O_2 is taken up by the primary enzyme in photorespiration. Increased C_3 photorespiration reduces net C_3 photosynthesis rates at higher temperature, while C_4 photosynthesis rates remain relatively constant across a wide range of leaf temperatures. This mechanism is the basis for using growing season air temperature in models of climatic effects on C_3 and C_4 productivity (Ehleringer et al., 1997; Collatz et al., 1998; Still et al., 2003). However, extending this leaf-scale effect to continental and global climate data is problematic because leaf temperature is a 'phylloclimatic' variable which shows temporal trends and spatial trends (between plants and within individual leaves) that differ significantly from trends in ambient air temperature (Chelle, 2005). Leaf temperature is problematic because at a given time and position, it depends not only on ambient air temperature, but also on factors of the leaf energy balance, as modelled in terms of a boundary layer climate (Oke, 1992):

$$T_\mathrm{l} = T_\mathrm{a} + \frac{r_\mathrm{b}}{k_\mathrm{a}}\left[Q^*_{(\mathrm{leaf})} - Q_{E(\mathrm{leaf})}\right], \tag{2}$$

where T is temperature (K), subscripts l for leaf, a for ambient air, r_b is the laminar boundary layer resistance (s m^{-1}), k_a is the volumetric heat capacity of air (J m^{-3} K^{-1}), Q is heat flux density J m^{-2} s^{-1}), * is for net all-wave radiation, the subscript E denotes for turbulent latent heat; both Q terms can be positive or negative. In fact, the only condition that results in $T_\mathrm{l} = T_\mathrm{a}$ is when the radiative heat flux equals the turbulent latent heat flux ($Q^*_{(\mathrm{leaf})} = Q_{E(\mathrm{leaf})}$). Considering this leaf energy balance, T_l will rarely equal T_a and will commonly be both moderated and cooled substantially by $Q_{E(\mathrm{leaf})}$ via transpiration (Chapin et al., 2002), especially during the growing season. Both T_a and T_l are directly dependent on the amount of total solar irradiance (Q_s) used in our calculation of W by way of energy partitioning into sensible and latent heat flux. Considering annual averages, the total radiation absorbed by plants will be partitioned primarily into $Q_{E(\mathrm{leaf})}$ and radiant (Q_R) and convective (Q_C) heat losses (neglecting a very small amount of biochemical heat storage by photosynthesis, and physical heat storage by plant matter (Gates, 1968). Q_R and Q_C account for the transfer of energy to changes in T_l, the mechanistic control on photosynthesis rates in the crossover temperature model (Ehleringer et al., 1997; Collatz et al., 1998; Still et al., 2003). Meanwhile $Q_{E(\mathrm{leaf})}$ is only accounted for by our consideration of transfer of solar energy to transpiration in W. Thus basing our model on W rather then T implicitly accounts for $Q_{E(\mathrm{leaf})}$, but also folds the effects of heat loss to convection and radiation into our calculation of W. Our model fully accounts for $Q_{E(\mathrm{leaf})}$ via transpiration and the ability of ecosystems to maintain T_l that differ and are more stable than T_a during the growing season. This model thereby reduces controls on C_3 versus C_4 productivity to a single variable (W expressed in mol H_2O m^{-2} yr^{-1}) and in doing so considers the complete water and energy balance of plants. W is derived from the same primary energy and water balance flux data as other continental-scale estimates of annual GPP and transpiration fluxes (Berry and Roderick, 2004). The model described here assumes that annual water use by an ecosystem is partitioned into C_3 and C_4 components via a relationship to GPP, and that each of those components has a distinct $\delta^{13}C_\mathrm{p}$ signature that is reflected in $\delta^{13}C_{SOC}$. We consider this approach to be superior to temperature-based models because although T_l may be a primary control on C_3 and C_4 net photosynthesis rates, it is difficult to measure on a continental or global basis, while W is readily derived from global climate data sets. Based on the results of our statistical analyses discussed below, we also prefer this foundation in mechanisms calculated from energy and water balance of plants, as opposed to air temperature-dependant models.

2.3.2. *Model description and methods.*

2.3.2.1. SOC inventory and C_4-derived SOC. In previous work, we showed that for this data set of Australian soils W is a good measure of the climatic control on the amount of SOC inventory in the absence of edaphic and biotic factors that inhibit SOC decomposition (Wynn et al., 2006). We use these assumptions to describe variation of SOC inventory (mol C m^{-2}) over some depth interval with respect to W (kmol H_2O m^{-2} yr^{-1}) in terms of a logistic function:

$$\mathrm{SOC} = f(W) = \frac{E_\mathrm{SOC}}{\Lambda + (E_\mathrm{SOC}/\mathrm{SOC}_\mathrm{min} - \Lambda)\,\mathrm{e}^{-E_\mathrm{SOC}W}}, \tag{3}$$

where E_SOC is the efficiency of SOC storage per unit W, and has dimensions of (mol C yr mol^{-1} H_2O). Λ is the density limitation of SOC inventory and has dimensions (m^2 yr mol^{-1} H_2O). Λ relates E_SOC to the maximum SOC inventory ($\Lambda = E_\mathrm{SOC}/\mathrm{SOC}_\mathrm{max}$; $\mathrm{SOC}_\mathrm{max}$ is analogous to carrying capacity in sigmoidal population growth functions). The function in eq. (3) describes a sigmoidal curve of SOC with respect to W and is shown in Curve (a) of Fig. 3. Above a threshold of W, SOC inventory approaches $\mathrm{SOC}_\mathrm{max}$. Below this threshold, SOC inventory is directly related to W by the slope ($\partial\mathrm{SOC}/\partial W$). The slope can be reduced to units of [(mol C mol^{-1} H_2O) × yr], showing its relevance as a measure of the efficiency of SOC storage per unit water availability. The dimension of time remains in the numerator because SOC is a reservoir, while W is a flux. To reduce the slope of

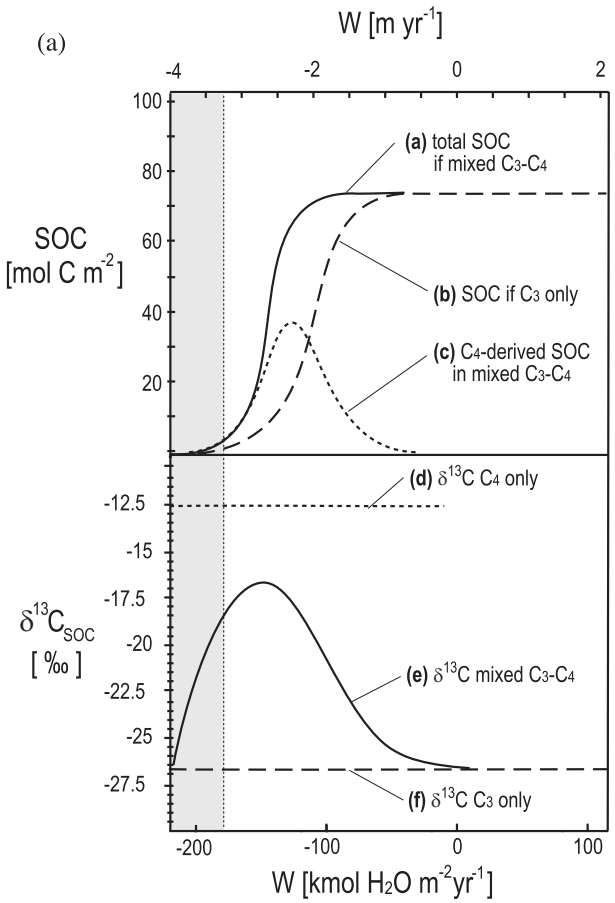

Fig. 3. Optimized water use efficiency model of SOC inventory in C_3, C_4 and mixed C_3–C_4 soils. (a–c) Model functions of SOC inventory with respect to water availability assuming two conditions: (a, c) Mixed C_3–C_4 vegetation (total, and SOC derived from C_4 plants), and (b) only C_3 vegetation. (d–f) Model functions of stable carbon isotopic composition of SOC with respect to water availability. Using the model functions (a–c) and model parameters of the carbon isotopic composition of plant biomass (d, f), the resultant isotopic composition of SOC in mixed C_3–C_4 soils (e) is calculated by mass balance. Model parameters shown are $E_{\mathrm{SOC}} = 5.61 \times 10^{-5}$ mol C yr mol^{-1} H_2O, $\Lambda = 5.35 \times 10^{-5}$ m^2 yr mol^{-1} H_2O, $\mathrm{SOC_{min}} = 0.537$ mol C m^{-2} (values from least-squares regression to the Australian SOC inventory data for 0–5 cm depth interval; Wynn et al., 2006). Additional model parameters shown are: $\delta_{C3} = -26.7‰$, $\delta_{C4} = -12.5‰$ (values of $\delta^{13}C_p$ from C_3 and C_4 plants from compilation of Cerling et al., 1998), and $\beta = 1.2$. Greyed area shows values of W below minimum W for Australia (-180 kmol H_2O m^{-2} yr^{-1}).

eq. (3) to units of water use efficiency (mol C mol^{-1} H_2O) we would need to know the mean turnover time of SOC to convert the SOC inventory to a mean C flux to soil.

Logistic functions such as eq. (3) can also be described in terms of maxima and minima and maximum slope. For our model function in eq. (3), an equivalent form in these terms is:

$$\mathrm{SOC} = f(W) = \frac{\mathrm{SOC_{max}}}{1 + [(\mathrm{SOC}_{TG,\max}/\mathrm{SOC_{min}}) - 1]\mathrm{e}^{-E_{\mathrm{SOC}}W}}, \quad (4)$$

where $\mathrm{SOC_{min}}$ and $\mathrm{SOC_{max}}$ are the minima and maxima, while E_{SOC} is the maximum slope. Thus E_{SOC} is a description of the water use efficiency of optimally competitive ecosystems comprising mixtures of C_3 and C_4 plants at delivering C to the SOC pool under current climatic conditions. E_{SOC} reflects $\mathrm{WUE_{ph}}$, but is modified by the fraction of GPP that is input to SOC during transformation of biomass C to SOC.

Curve (b) in Fig. 3 shows a similar logistic function of SOC with respect to W under conditions where only C_3 photosynthesis occurs. This curve is modified from Curve (a) considering that C_4 plants are known to be more water use efficient than C_3 plants (see Section 2.3.1). We modify eq. (4), dividing E_{SOC} by a dimensionless number (β) describing the theoretical ratio of E_{SOC} for C_4 and C_3 plants:

$$E_{\mathrm{SOC}(C_3)} = \frac{E_{\mathrm{SOC}}}{\beta}. \quad (5)$$

Thus, the only difference between the two curves is the lower maximum slope (E_{SOC}) for C_3 plants due to their lower $\mathrm{WUE_{ph}}$.

Curve (c) in Fig. 3 is simply the difference between curves (a) and (b), and is thus the additional inventory of SOC that results from allowing C_4 photosynthesis to occur in water limited environments. The function describing this inventory of C_4-derived SOC is:

$$\begin{aligned}\mathrm{SOC_{C_4}} &= \mathrm{SOC_{total}} - \mathrm{SOC_{C_3}} \\ &= \frac{E_{\mathrm{SOC}}}{\Lambda}\left[\frac{1}{1 + (\mathrm{Z} - 1)\,\mathrm{e}^{-E_{\mathrm{SOC}}W^*}}\right. \\ &\quad \left. - \frac{1}{1 + (\mathrm{Z} - 1)\,\mathrm{e}^{-E_{\mathrm{SOC}}W^*/\beta}}\right], \end{aligned} \quad (6)$$

where

$$\mathrm{Z} = \frac{E_{\mathrm{SOC}}}{\Lambda \mathrm{SOC_{min}}} = \frac{\mathrm{SOC_{max}}}{\mathrm{SOC_{min}}}. \quad (7)$$

The modelled inventory of C_4-derived SOC shows an optimum in the area between Curves (a) and (b). C_4-derived SOC decreases left of the optimum value, due to extremely low W (although C_4-derived SOC is the majority of the total SOC for the low values of W in this region). C_4-derived SOC also decreases to the right of the optimum value due to increased competition by C_3 photosynthesis at higher W.

2.3.2.2. Stable carbon isotope values of SOC from mixed C_3–C_4 ecosystems. Using the functions for SOC inventory described in Section 2.3.2.1, and values for the stable carbon isotopic composition of C_3- and C_4-derived SOC ($\delta^{13}C_{C_3}$, $\delta^{13}C_{C_4}$), we use mass balance to derive a mixing equation for the carbon

isotopic composition of total SOC:

$$\delta^{13}C_{SOC} = \frac{SOC_{C_3}\delta_{C_3} + SOC_{C_4}\delta_{C_4}}{SOC}$$
$$= [1 + e^{-E_{soc}W}(Z-1)]\left\{\frac{\delta_{C_3}}{1+(Z-1)e^{-E_{soc}W/\beta}} - \delta_{C_4}\left(\frac{1}{1+(Z-1)e^{-E_{soc}W/\beta}} - \frac{1}{1+(Z+1)e^{-E_{soc}W}}\right)\right\}. \quad (8)$$

An example of this function with constant $\delta^{13}C_{C_3}$ and $\delta^{13}C_{C_4}$ is shown in Curve (e) of Fig. 3. This model function of water use efficiency is applied to data from our measurements of $\delta^{13}C_{SOC}$ across the range of climates representative of the continental scale of Australia. Non-linear least-squares regression was performed using ANOVA analysis with mathematical modelling software (Mathematica©), with data weighted according to the inverse of errors measurements between transects.

2.3.2.3. Model parameters. The model parameters used in our analysis include $\delta^{13}C$ values from C_3 and C_4 plants derived from a large data set (Cerling et al., 1997; $\delta^{13}C_{C_3} = -26.7 \pm 2.7‰$, $\delta^{13}C_{C_4} = -12.5 \pm 1.1‰$, 1σ standard deviation). In some model runs, we used constants while in others we used two sigmoidal functions to estimate the natural variation of $\delta^{13}C_p$ with respect to W within each photosynthetic pathway (C_3 equation here, C_4 equation follows a similar form):

$$\delta^{13}C_{C_3} = f(W) = \delta_{mean(C_3)} + \frac{1}{2}\delta_{range(C_3)} - \frac{\delta_{range(C_3)}e^{\frac{5\left[W-1/2\left(W_{max\,C_3}+W_{min\,C_3}\right)\right]}{W_{max\,C_3}-W_{min\,C_3}}}}{1+e^{\frac{5\left[W-1/2\left(W_{max\,C_3}+W_{min\,C_3}\right)\right]}{W_{max\,C_3}-W_{min\,C_3}}}}, \quad (9)$$

where $\delta^{13}C_{C_3}$ is the carbon isotopic composition of living biomass as a function of W, $\delta_{mean(C_3)}$ and $\delta_{range(C_3)}$ are the mean and range of average compositions for the pathway. $W_{min\,C_3}$ and $W_{max\,C_3}$ are values at which $\delta^{13}C_{(C_3)}$ 'turns over' towards a maximum and minimum (the maximum change in slopes of the sigmoidal curve). Based on observational constraints in this data set, we use the following values to describe variation of $\delta^{13}C_p$: $W_{min\,C_3}$ of -180 kmol H_2O m^{-2} yr^{-1} from the point at which SOC approaches 0 (W below -183 kmol H_2O m^{-2} yr^{-1} does not occur in Australia), $W_{max\,C_4} = -120$ kmol H_2O m^{-2} yr^{-1} from the point at which SOC approaches a maximum in this data set (plant metabolism becomes energy limited, and hence SOC storage reaches a maximum), $W_{max\,C_3} = -55$ kmol H_2O m^{-2} yr^{-1} from the point at which actual evaporation approaches potential evaporation, and beyond which evaporation is limited by energy rather than by water supply (evaporation becomes energy limited; Berry and Roderick, 2002a). Mean $\delta^{13}C_{SOC}$ values derived from C_4 plants are always offset by $+14.2‰$ with respect to $\delta^{13}C_{SOC}$ derived from C_3 plants.

We used several versions of these sigmoidal functions to describe the relationship between W and $\delta^{13}C_p$ for C_3 and C_4 plants. The positive correlation between Δ_B and water availability in C_3 plants is well documented from both theoretical and observational perspectives (plants under drought stressed conditions in arid climates discriminate less against ^{13}C, and thus have more ^{13}C-enriched $\delta^{13}C_p$ values; Farquhar et al., 1982a, b, 1988; Winter et al., 1982; Farquhar and Richards, 1984; Brugnoli et al., 1988; Ehleringer, 1993). For example C_3 plants in arid regions of East Africa average $\sim -24.6‰$, while those in open canopy forests average $\sim -27.8‰$ and closed canopy forests average $\sim -31.4‰$ (Cerling et al., 2003). Although some previous work has suggested that physiological discrimination in C_4 plants is negligible, Buchmann et al. (1996) demonstrated a negative correlation between Δ_{B-C_4} and water supply across biochemical subtypes of C_4 grasses (mesic grasses using NAPD pathways have $\delta^{13}C_p$ values of $-11.8 \pm 0.2‰$ and xeric grasses using NAD and PCK pathways have $\delta^{13}C_p$ values of $-13.1 \pm 0.3‰$; Cerling et al., 2003). Based on these observations, we modelled the natural variation of $\delta^{13}C_p$ of C_3 and C_4 plants with respect to W using a variety of combinations of the sense of correlation or lack of correlation: (1) positive relationship between Δ_B for both C_3 and C_4, (2) no relationship for either C_3 or C_4, (3) positive relationship for C_3, none for C_4 and (4) positive relationship for C_3, negative for C_4.

2.3.3. Model simplifications. Equation (7) takes into account differences in the rate of C assimilation via C_3 and C_4 photosynthesis into the SOC pool. These differences are modelled as differences in mean E_{SOC} of each plant group, following differences in WUE_{ph}. The model assumes no difference in the rate of decomposition of C_3- versus C_4-derived SOC. We also assume that mean annual decomposition rate depends primarily on mean annual soil temperature, and not on W, and thus is not part of the simple analytical model. Our model considers only the bulk soil $\delta^{13}C_{SOC}$ and makes the assumption that the bulk pool is the mass weighted average of the spectrum of pools of SOC integrated over its spectrum of turnover times (Trumbore, 1997). The model also does not account for differences in N use efficiency or availability of N or other nutrients. In our analysis of climatic controls, we avoid these edaphic effects by limiting the data to coarse-textured soils (<10% fine particles <63 μm diameter) for which nutritional status is relatively constant due to a narrow and limited range of cation exchange capacity (CEC) of sands (Brady and Weil, 2002). This simplification of the model thereby assumes that N availability follows the same environmental controls as water availability—a reasonable assumption because N uptake in low CEC soils is limited by solubility and water uptake rate. The simplified model likewise avoids the bulk of other potential edaphic controls on $\delta^{13}C_{SOC}$ because it is based

on measurements of a consistently sampled depth interval near the surface (0–5 cm depth), which is a good representation of the most labile pool of SOC. To justify this simplification, we later consider a sample set from a deeper pool of SOC (5–25 cm depth), and particle size separates to separately examine the edaphic and biotic controls on $\delta^{13}C_{SOC}$ from samples that span these environmental gradients.

Because our model is based entirely on differences in E_{SOC}, it does not consider the long-term effects of changes in atmospheric pCO_2, which is relatively well mixed (varying by only $\sim$2–3 μmol mol^{-1} in the tropical latitudes where C_4 plants exist; Bolin and Keeling, 1963). Temporal changes in pCO_2 since the Industrial Revolution have caused a 1.5‰ ^{13}C-depletion of organic carbon since that time. The increase in atmospheric CO_2 may have driven decreases in the proportion of C_4 plants via CO_2 fertilization of 'mesic' plants (Berry and Roderick, 2002b) which are less water use efficient and mostly use C_3 photosynthesis (Farquhar, 1997). By reducing our analysis to the surface (0–5 cm depth) sampling interval in coarse textured soils, and thus to the most labile pool of SOC, we have eliminated the effect of such long-term temporal changes in vegetation to the degree that is possible.

3. Results and discussion

3.1. Measurements of the stable carbon isotopic composition of Australian SOC

Stable carbon isotope ratio data of bulk soil used in this study are presented in an online supplement to our paper discussing environmental controls on SOC inventory at the continental scale (Wynn et al., 2006). $\delta^{13}C_{SOC}$ from the 0–5 cm depth interval sampled near trees (−T, 'tree' samples) ranged from −29.4 to −20.9‰, while $\delta^{13}C_{SOC}$ values from the same interval away from trees (−G, 'grass' samples) ranged from −29.4 to −17.5‰. The −TG weighted values (mathematically apportioned −T and −G values using measurements of fractional canopy cover) range from −29.4‰ to a maximum of −18.2‰. All soil regions with a fractional canopy cover greater than 0.5 (mostly closed canopy vegetation consisting predominantly of C_3 biomass) showed −TG weighted $\delta^{13}C_{SOC}$ values more ^{13}C-depleted than −23.2‰. All soil regions where the index of annual water availability (W) was greater than −120 kmol H_2O m^{-2} yr^{-1} showed $\delta^{13}C_{SOC}$ values more ^{13}C-depleted than −23.9‰, consistent with C_3-dominated vegetation ($\delta^{13}C$ values above $\sim$ −24‰ are consistent with some proportion of C_4 biomass). Most surprisingly, the most ^{13}C-enriched $\delta^{13}C_{SOC}$ value our data set, which never extends above −17.5‰, even for −G sampling locations, was not as ^{13}C-enriched as typical pure C4 biomass (−12.5‰), or even the ^{13}C-depleted end member of C_4 biomass (−13.6‰).

3.2. Examination of the environmental controls on Australian SOC stable isotopic composition

Many of the environmental variables potentially controlling the $\delta^{13}C_{SOC}$ are highly intercorrelated (Table 1), prompting the use of factor analysis to reduce the number of fundamentally controlling variables analysed (Fig. 2). In our factor analysis, we found that greater than half (59%) of the variance among regions is described by component 1, which is comprised mainly of factors related to precipitation, primary productivity and the proportion of woody vegetation (Table 2; MAP, 1/VPD, W, ndvi and f_w). Component 2 accounted for 16% of the variance and was mainly correlated with *MAT* (Table 2), and weakly correlated with the inventories of SOC and N, and fine mineral particles (<63 μm). This factor analysis and a number of previous observational studies (Bird and Pousai, 1997; Bird et al., 2002a, b, 2003) suggest that some combination of MAP and MAT may provide a good prediction of climatic control on $\delta^{13}C_{SOC}$. Other previous studies of the climatic control on the distribution of C_3 and C_4 grasses has emphasized the role of growing season air temperature as a good predictor of $\delta^{13}C_p$ (Teeri, 1988; Ehleringer et al., 1997), presumably because it is a good predictor of growing season leaf temperature as discussed above. However, we found a poor correlation between MAT and $\delta^{13}C_{SOC}$ and that a correlation between growing season T_a and $\delta^{13}C_{SOC}$ is only obvious for the

Table 1. Correlation coefficients for environmental data ($n = 48$)

	f_w	MAT	MAP	ndvi	W	$f_{<63\,\mu m}$	pH	SOC	N	1/VPD
f_w	1	−0.170	0.744	0.839	0.780	−0.292	−0.572	0.712	0.512	0.668
MAT		1	−0.196	−0.179	−0.411	−0.372	0.025	−0.480	−0.337	−0.605
MAP			1	0.728	0.935	−0.181	−0.657	0.715	0.267	0.761
ndvi				1	0.782	−0.342	−0.556	0.727	0.414	0.718
W^*					1	−0.215	−0.624	0.851	0.416	0.925
$f_{<63\,\mu m}$						1	0.283	−0.111	−0.052	−0.195
pH							1	−0.535	−0.070	−0.537
SOC								1	0.646	0.867
N									1	0.522
vpd										1

Table 2. Rotated component matrix for factor analysis

	Component	
Variable	1	2
f_w	0.882	0.023
MAT	−0.219	−0.871
MAP	0.886	0.042
ndvi	0.888	−0.005
W	0.935	0.221
$f_{<63\,\mu m}$	−0.416	0.659
pH	−0.740	0.232
SOC	0.844	0.403
N	0.462	0.477
1/VPD	0.856	0.402

warmest growing season environments of our data set (Fig. 2). This may be because growing season T_a does not account for the moderation of T_l by latent heat flux via transpiration. These statistical analyses suggests that climatic variables contributing to water and energy balance of plants (VPD, W) during assimilation are likely to produce a better predictor of $\delta^{13}C_{SOC}$, and hence of $\delta^{13}C_p$ and of the spatial distribution of C_3 and C_4 plants under natural environmental conditions.

Given these observations, we used repeated stepwise linear regression to examine the primary environmental variables controlling $\delta^{13}C_{SOC}$. This analysis revealed two dominant, but very well correlated climatic factors both of which are based on the availability of water to plants for metabolic processes (W and VPD). Either of these derived variables individually accounts for the combined effects of MAP and MAT evident in our factor analysis (Fig. 2; Table 2). We chose W as the primary variable to formulate the optimized water use efficiency model because of its ease of use, and reduction to units of amenable to the interpretation of plant water use and water use efficiency (i.e. annual flux in kmol H_2O m^{-2} yr^{-1}, see previous discussion of optimized water use efficiency model of SOC).

After the variance of $\delta^{13}C_{SOC}$ due to W or VPD was removed, the proportion of fine mineral particles ($\leq$63 μm diameter) remained the only significant correlation (p <0.05). Other non-climatic factors such as N availability, litter quality, pH, and clay content have been isolated in our data analysis such that they are either minor secondary controls compared to W, or are well correlated to W (Table 2). This result suggests that W can fully account for all climatic controls on $\delta^{13}C_{SOC}$, and presumably climatic controls on the distribution of C_3 and C_4 plants.

3.3. *Estimating model parameters: climatic controls on Australian SOC stable isotopic composition*

Using the optimized water use efficiency of SOC model described above, we allowed $\delta^{13}C_p$ and β values to vary in our regression analysis of this data set to the model function, to account for environmental differences in $\delta^{13}C_p$ input to the SOC pool (Fig. 4). Four models are shown using a variety of combinations of the sense of the relationship between $\delta^{13}C_p$ and W for C_3 and C_4 plants. For the single model in which the average $\delta^{13}C_p$ values of C_3 and C_4 plants was held constant across climates (Fig. 4a), the regressed value of $\delta^{13}C_{SOC}$ derived from C_3 plants was −27.7‰, and β was 1.194. For the three models in which the natural variation of $\delta^{13}C_p$ in C_3 plants is correlated to W (Figs. 4b–d), best fit regressions of eq. (8) to the data set were very similar and produced regressed values of $\delta^{13}C_{SOC}$ derived from C_3 plants, ranging from −25.5‰ to −25.6 ‰. For this group of model runs, the calculated ratio of the efficiencies of SOC storage for C_4 to C_3 ecosystems (β) were also very similar and ranged from 1.058 to 1.064. For the latter three model runs shown, this simple relationship to the single variable explains more than 85% of the variance observed in the entire data set.

Using our model of optimized water use efficiency of SOC production, we calculated ratio of water-use advantage of C_4 plants as:

$$\mathrm{WUA}_{C_4/C_3} = \frac{E_{SOC,C_4}}{E_{SOC,C_3}} = \frac{\partial \mathrm{SOC}_{C_4}/\partial W}{\partial \mathrm{SOC}_{C_3}/\partial W}$$

$$\mathrm{WUA}_{C_4/C_3} = \frac{\beta\left[1+\frac{(Z-1)}{e^{E_{SOC}W\beta^{-1}}}\right]^2}{e^{E_{SOC}W(1-\beta^{-1})}\left[1+\frac{(Z-1)}{e^{E_{SOC}W}}\right]^2}, \quad (10)$$

where WUA_{C_4/C_3} is the 'water use advantage' of C_4 plants over C_3 plants in assimilating C in the SOC pool. This dimensionless number is thus greater than unity for conditions where C_4 plants are more water-use efficient than C_3 plants. WUA_{C_4/C_3} is greater than unity up to −135 kmol H_2O m^{-2} yr^{-1} W, showing the range of environments over which C_4 plants have a water-use advantage over their C_3 counterparts in mixed ecosystems (below −135 kmol H_2O m^{-2} yr^{-1} W with a maximum advantage at −171 kmol H_2O m^{-2} yr^{-1} W, Fig. 5).

Building on the model function of optimized water use efficiency of SOC storage, we infer *MAT* to be the primary control on SOC decomposition rates based on previous observational and modelling studies (Berg et al., 1993; Lloyd and Taylor, 1994; Kirschbaum, 1995; Trumbore, 1997, 2000a, b; Kätterer et al., 1998; Lenton and Huntingford, 2003; Liski et al., 2003; Sanderman et al., 2003). Mean turnover time of the bulk SOC pool in this model affects $\delta^{13}C_{SOC}$ by way of the terrestrial Suess effect which has progressively depleted SOC of ^{13}C by ∼1.5‰ since the Industrial Revolution (Bird et al., 1996). Accounting for this effect with a simple linear relationship, the isotopic composition of SOC in the 0–5 cm pool can be described in terms of two simple climatic variables as:

$$\delta^{13}C_{SOC} = f(W) - k\,(\mathrm{MAT}). \quad (11)$$

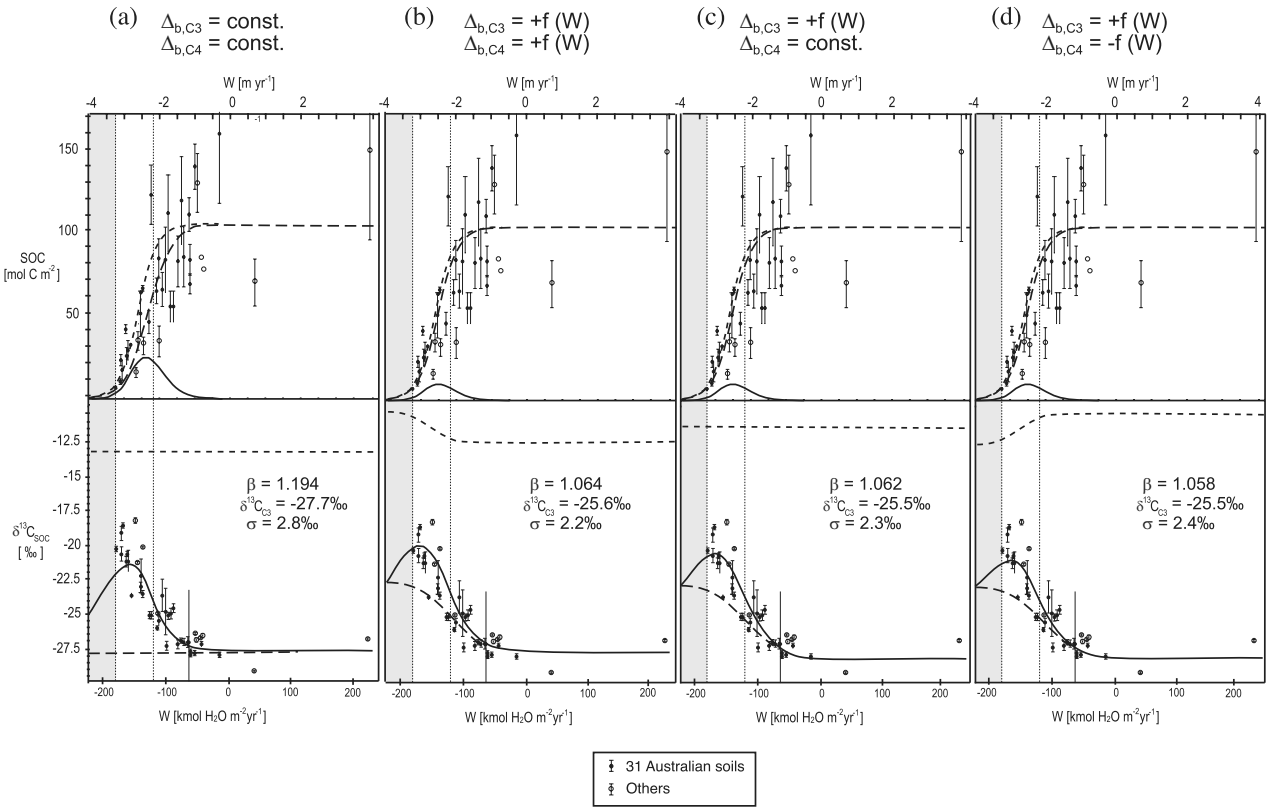

Fig. 4. Application of the model in Fig. 3 to $\delta^{13}C_{SOC}$ and SOC inventory data from the 0–5 cm depth interval. Thresholds shown as in Fig. 2. (a) no relationship between Δ_B and W for either C_3 or C_4, (b) positive relationship for both C_3 and C_4, (c) positive relationship for C_3, none for C_4, and (d) positive relationship for C_3, negative for C_4. Greyed area shows values of W below minimum W for Australia (-180 kmol H_2O m^{-2} yr^{-1}). Two thresholds of W are shown with vertical dashed lines on each plot: -120 kmol H_2O m^{-2} yr^{-1} W, above which SOC inventory is not limited by W, and at -55 kmol H_2O m^{-2} yr^{-1} W, above which evaporation is not limited by W.

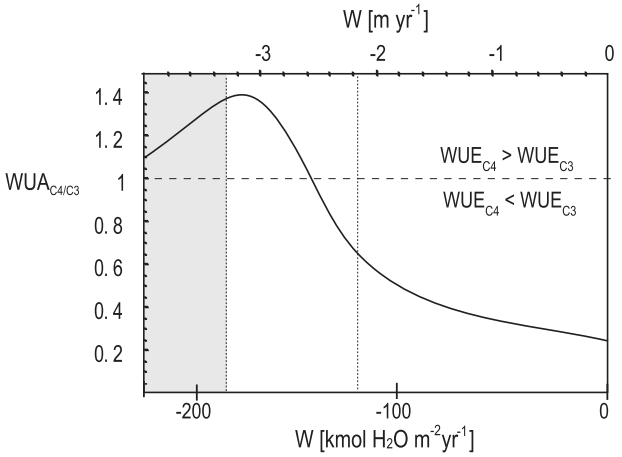

Fig. 5. Modelled water-use advantage of C_4 plants over C_3 plants (WUA_{C_4/C_3}) with respect to the index of annual water availability (W) using data from this study. Thresholds shown as in Fig. 2.

A linear regression of the residual from the $\delta^{13}C_{SOC}$ relationship to W has a slope of -0.071‰/K, and thus a total magnitude of 1.1‰ for the Australian data set (15.9 K range of MAT).

3.4. *Interpreting model parameters: the carbon isotopic composition of the continental scale SOC pool*

Our regressed mean values of $\delta^{13}C_{SOC}$ for C_3 and C_4 ecosystems (-25.3 and -11.1‰) are slightly more ^{13}C-enriched than measurements of mean biomass from large global data compilations (by 1.4‰, as compared to the compilation of Cerling et al., 1998). This ^{13}C enrichment in our data set is likely due to a combination of factors. $\delta^{13}C_{SOC}$ may be ^{13}C-enriched with respect to average modern biomass due to a greater representation of input to SOC from root-derived rather than leaf-derived litter, since the former is generally ^{13}C-enriched by about 1.5‰ (Brugnoli and Farquhar, 2000). We note however that we have minimized this effect by using the shallowest sampling interval (0–5 cm, the 5–30 cm depth interval is on average 1.3‰ more ^{13}C-enriched, but shows the same climatic trends with respect to W). Also, because most C_3 plants in Australia are evergreen, and evergreen plants are slightly more ^{13}C-enriched than deciduous varieties, typically by ∼1‰ (Stuiver and Braziunas, 1987; Farquhar et al., 1989; DeLucia and Schlesinger, 1991; Ehleringer et al., 1993; Marshall and Zhang, 1994), this may account for up to 1‰ of the difference between the regressed Australian $\delta^{13}C_{SOC}$ values

and mean $\delta^{13}C_p$ from more inclusive global plant data sets. And finally, despite our attempt to collect the most 'fresh' SOC by using the 0–5 cm depth interval from sandy soils only, and thereby minimize the effects of pedogenic processes on $\delta^{13}C_{SOC}$, this interval is still an average of input from $\delta^{13}C_p$ over the mean residence time of the 0–5cm pool (~1–30 yr). Therefore, the terrestrial Suess effect may account for some portion of our more ^{13}C-enriched SOC data as compared to typical biomass, up to a maximum of 1.5‰ (the maximum effect would only be reached if the mean age of the 0–5 cm pool were > 150 yr).

The relatively good fit of our $\delta^{13}C_{SOC}$ data to our model function emphasizes the role of WUE_{ph}, and the total water and energy balance of plants on C_3 and C_4 productivity under water limited climatic conditions typical of most of Australia. Although the gain in A per unit E may seem vanishingly small in well-watered environments, the marginal cost of photosynthesis becomes increasingly significant under water stressed conditions typical of the growing season in most of Australia. For example, Berry and Roderick (2004) estimated that at the scale of the Australian continent, each mole of CO_2 fixed by C_3 plants is accompanied by 175 mole of H_2O of transpiration. At current mean annual continental assimilation rates (73.3 mol CO_2 m^{-2} yr^{-1}), the authors also calculated that continental transpiration would be approximately 12.9 kmol H_2O m^{-2} yr^{-1}. The effect of this transpiration flux on the plant energy balance would amount to 580 MJ m^{-2} yr^{-1} of annual latent heat flux from plants. From these calculations, it is clear that transpiration is a significant component of the annual average water and energy balance of plants, and therefore must have a considerable effect on T_l. Mean annual continental transpiration flux amounts to nearly half the mean annual MAP flux (~25 kmol H_2O m^{-2} yr^{-1}), and approximately 7.5% of the mean annual Q_s flux (7.6 GJ m^{-2} yr^{-1}, which would amount to 170 kmol H_2O m^{-2} yr^{-1} if all Q_s flux were converted into latent heat of evaporation). These statistics would be much higher for the growing season, during which A and E are higher. The resulting effect on growing season T_l would be more pronounced than on these annual statistics.

Although we find that W has the most fundamental control on $\delta^{13}C_{SOC}$, regression of our model function (eq. 8) to W alone shows some residual relationship to *MAT*. Temperature dependence of biomass decomposition rates exerts some control over $\delta^{13}C_{SOC}$ through variable incorporation of the terrestrial Suess effect into the SOC pool (total maximum magnitude ~1.5‰). Our relationship to W performs well in accounting for $\delta^{13}C$ differences of input to SOC. However, rates of SOC decomposition are primarily controlled by temperature (Berg et al., 1993; Lloyd and Taylor, 1994; Kirschbaum, 1995; Trumbore, 1997, 2000a, b; Kätterer et al., 1998; Lenton and Huntingford, 2003; Liski et al., 2003; Sanderman et al., 2003). Soil temperature drives the observed latitudinal gradients in turnover time (Bird et al., 2002a), and hence the magnitude of the terrestrial Suess effect observed in the SOC pool. If mean SOC residence time increases with decreasing MAT, there is likely some variation of the magnitude of the terrestrial Suess effect observed in any bulk pool of SOC. Our linear regression constant, k in eq. (11) accounts for this variation. Thus the isotopic composition of SOC in the 0–5 cm pool can be attributed (as in eq. 11) to variation due to both W and MAT effects on turnover time represented by the terrestrial Suess effect. It is worth noting that a portion of the terrestrial Suess effect on $\delta^{13}C_{SOC}$ values may have already been accounted for by W, as our model function may incorporate some of the effect of water availability on decomposition rates (Meentemeyer, 1978). Using this more complete model of water and energy balance control on plant water use efficiency, combined with temperature control on turnover time, and with our stable isotope data from Australian SOC we obtain the following model values: $\beta = 1.108$, $\delta^{13}C_{p(C_3)} = -24.7$‰ (mean, actual function of W described by a positive relationship in eq. 9), $\delta^{13}C_{p(C_4)} = -10.5$‰ (mean, actual function of W described by a positive relationship in eq. 9), $k = -0.071$ K^{-1}, $Z = 163$ mol C m^{-2} and $E_{SOC} = 5.61 \times 10^{-5}$ mol C yr mol^{-1} H_2O. This regression equation, which follows physically realistic model parameters, and is based on two simple environmental variables, explains 92% of the variance observed in the entire $\delta^{13}C_{SOC}$ data set. This model based solely on differences in the water use efficiency of C_3 and C_4 plants explains the observed variance of $\delta^{13}C_{SOC}$ better than any relationship to *MAT* or growing season temperature (mean temperature during the wettest quarter year; Fig. 6). Growing season air temperature is a relatively good approximation of $\delta^{13}C_{SOC}$, but only in the warmest growing season environments of our data set. Growing season air temperature does not account for the deviation of T_l from T_a, and hence cooling by latent heat flux of transpiration. Thus the water-use efficiency model accounts for all major climatic variables contributing to water and energy balance during photosynthesis using a simple reduced variable, W. Although this model accounts for C_3 and C_4 plant distribution in deserts and savannas where water use efficiency is the dominant mechanistic control, we expect that our model would perform poorly at accounting for variability in $\delta^{13}C_{SOC}$ in temperate and boreal regions (above ~0 kmol H_2O m^{-2} yr^{-1} W). We have few validating data collected from these regions using the same protocol in order to test this performance.

Our model calculations relate to the differences in average E_{SOC} of mixed C_3–C_4 ecosystems, and not to individual C_4 versus C_3 plants. In a given environment, plants of both types may have different adaptive capabilities for coping with water stress. For example, in a mixed C_3–C_4 savanna, C_3 trees may utilize deeper root systems to tap into deeper water sources, while the C_4 plants may benefit from more efficient use of surface soil water, and C_4 plants may have different adaptive strategies to utilize their lower leaf-to-air CO_2 concentration gradients. Plants with each of these strategies within an ecosystem may contribute differently to annual GPP, and thus to SOC storage.

It is surprising to note the overall low proportion of C_4-derived SOC, even in the most open savanna grassland environments (Fig. 7a), and the most arid climates (Fig. 4). In our entire data

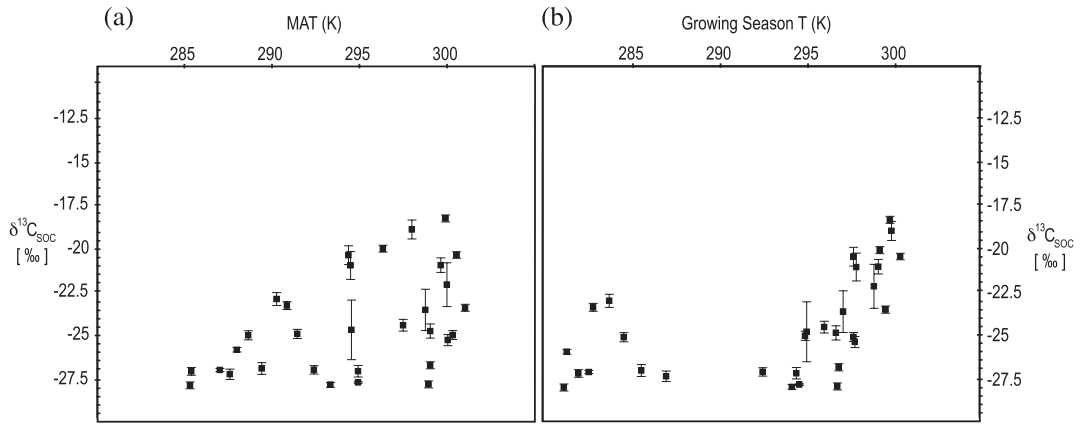

Fig. 6. Stable carbon isotope composition of soil organic carbon ($\delta^{13}C_{SOC}$) with respect to (a) mean annual temperature (MAT) and (b) mean growing season temperature for the regions studied. Growing season temperature is estimated as the mean temperature during the wettest quarter of the year.

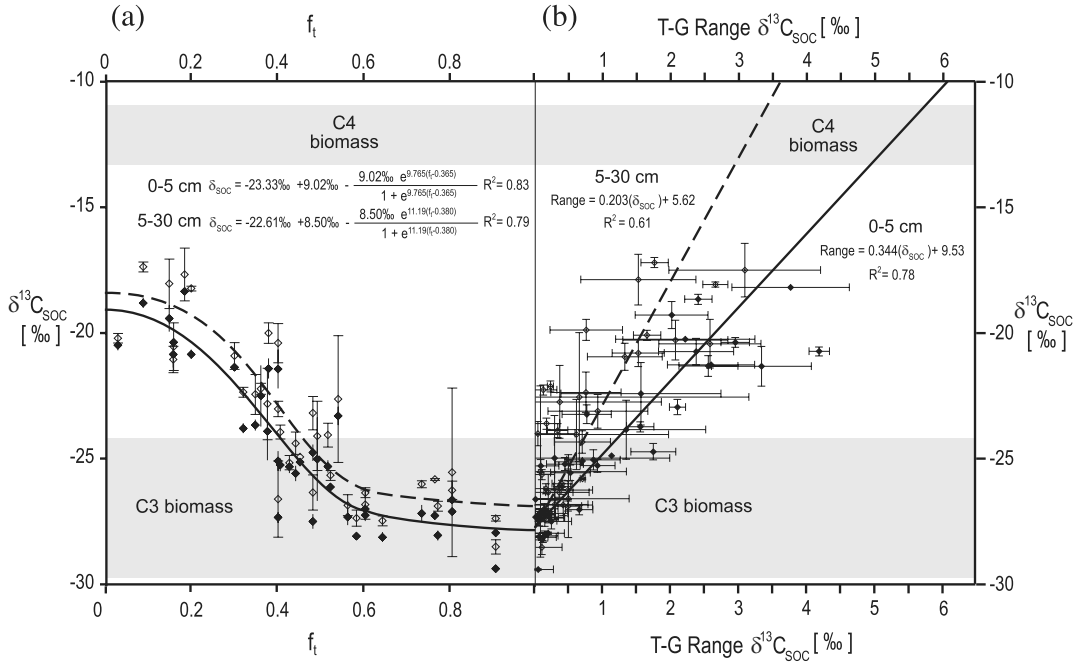

Fig. 7. (a) Stable carbon isotope composition of soil organic carbon ($\delta^{13}C_{SOC}$) with respect to the fractional canopy cover estimates from the data set in this study (f_t). (b) The range of $\delta^{13}C_{SOC}$ values between average of 25 'tree' and 'grass' sampling locations for each region in this study with 'tree' and grass locations with respect to bulk soil $\delta^{13}C_{SOC}$. Grey areas show typical mean and standard deviation of C_3 and C_4 biomass (from compilation of (Cerling et al., 1998). Closed symbols: 0–5 cm depth interval; open symbols: 5–30 cm depth interval.

set of 0–5 cm depth in sandy soils, $\delta^{13}C_{SOC}$ is always more ^{13}C-depleted than −18‰ while the 5–30 cm depth interval is always more depleted than −17‰. Even the 'grass' samples are never more ^{13}C-enriched than −17.5 and −17‰. The fact that $\delta^{13}C_{SOC}$ never reaches ^{13}C-enriched values typical of C_4 biomass suggests one of three possibilities: (1) greater primary productivity of C_3 biomass in open-canopy environments (which would contradict observations of lower WUE_{ph} of C_3 plants), (2) selective preservation of components of both C_3 and C_4 plants that are more ^{13}C-depleted than bulk biomass (although most $\delta^{13}C_{SOC}$ values in C_3 environments are more ^{13}C-enriched than typical C_3 plants), or more likely and (3) selective preservation of C_3-derived biomass as SOC in mixed C_3–C_4 ecosystems (Wynn & Bird, 2007). Because we consider only sandy soils (predominantly unreactive silica) in this analysis, the selective preservation of components of organic matter by fine particles and aggregates (Amelung et al., 1999) is assumed to be a minor contribution. Selective preservation of C_3-derived biomass in soil may operate due to (1) the more substantial input to SOC from C_3 roots, which penetrate the soil more deeply, or

are more extensive, (2) the selective preservation of C_3-derived woody biomass in a stable pool of charcoal and black C, (3) the preferential loss of C_4-derived C during biomass burning and/or grazing, or due to the CO_2 fertilization effect and (4) a difference in the turnover time of C_3- and C_4-derived SOC due to differences in the quality of organic matter (attributable in part to differences in lignin content), or some combination of (1–4).

Although we recognize that climatic, biotic and edaphic controls on $\delta^{13}C_{SOC}$ are interrelated, the aim of this analysis was to limit the factors influencing $\delta^{13}C_{SOC}$ to simple climatic variables by excluding some of the confounding effects of variations in biotic and edaphic conditions. In the following sections, we separately examine the potential effects of biotic and edaphic controls using the systematically collected data set.

3.5. Biotic controls on SOC stable isotopic composition

Figure 7a demonstrates a sigmoidal variation of $\delta^{13}C_{SOC}$ to measurements of the fractional cover of woody vegetation (f_t). Our stratified measurements of $\delta^{13}C_{SOC}$ are apportioned mathematically using the mean value of f_t over the 25 sampling locations. $\delta^{13}C_{SOC}$ is therefore sensitive to our f_t measurements, which vary with W (Fig. 8). We describe these relationships with an empirical least-squares regression of the bulk $\delta^{13}C_{SOC}$ as a function of f_t:

$$\delta_{SOC}(f_t) = \delta_{mid} + \frac{1}{2}\delta_{range} - \frac{\delta_{range} e^{s(f_t - f_{w\,mid})}}{1 + e^{s(f_t - f_{w\,mid})}}, \quad (12)$$

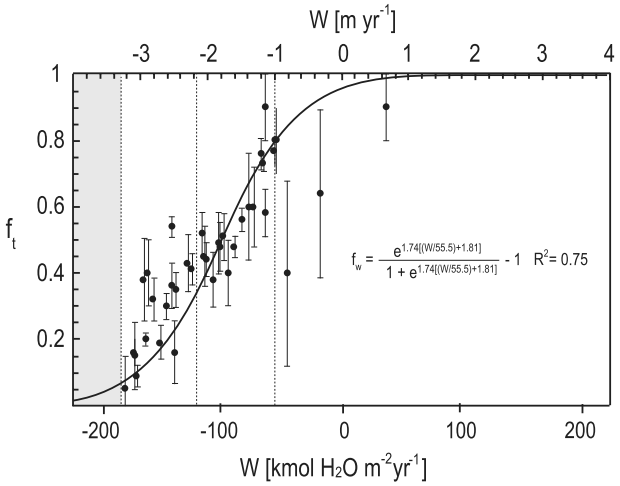

Fig. 8. Variation in the fractional canopy cover (f_t) measured for soil regions with 'tree' and 'grass' sites with respect to the annual moisture availability index (W). Regression equation describes a sigmoidal relationship with fixed variation between 0 and 1, with the lower 'turning value' fixed at -180 kmol H_2O m^{-2} yr^{-1} W, and the upper value set by least-squares regression at -20 kmol H_2O m^{-2} yr^{-1} W; units of W in the regression are in kmol H_2O m^{-2} yr^{-1}. Thresholds shown as in Fig. 2.

where δ_{mid} and δ_{range} describe the midpoint and range of predicted $\delta^{13}C_{SOC}$ values, $f_{t\,mid}$ and s describe the midpoint and maximum slope of the sigmoid.

From this relationship, it is expected that future research can provide more rigorous predictions of the proportion of trees and grass in savanna environments commonly used in palaeoenvironmental analysis based on $\delta^{13}C$ measurements from fossil soils (paleosols) in mixed C_3–C_4 ecosystems (savannas, e.g. Cerling, 1992a). Much of this work has predicted a proportion of canopy cover from $\delta^{13}C$ of soil components derived from biomass (organic matter and carbonate), using a simple mixing model between inputs from woody vegetation (predominantly C_3) and tropical grasses (predominantly C_4) to interpret the canopy cover of woody vegetation (Cerling et al., 1989; Quade and Cerling, 1995; Koch, 1998; Levin et al., 2004; Wynn, 2004), which is likely not as precise as the above analysis based on extensive data collected along extreme environmental gradients.

Figure 7b also demonstrates a significant relationship in the range of $\delta^{13}C_{SOC}$ values between equivalent 'tree' and 'grass' samples from the same region (T-G range $\delta^{13}C_{SOC}$), and the bulk $\delta^{13}C_{SOC}$ value within both depth intervals of this data set. This observation supports the argument that spatial variability of the distribution of C_3–C_4 biomass increases in arid environments (Wynn, 2004), a factor which should be taken into account in sampling and analysis of palaeoenvironmental reconstructions from palaeosols. The 5–30 cm depth interval shows a more similar $\delta^{13}C_{SOC}$ between tree and grass locations, again suggesting selective preservation of C_3-derived biomass as SOC in this depth interval, which has a longer mean residence time than the 0–5 cm interval.

3.6. Edaphic controls on SOC stable isotopic composition

Figure 9 shows variation of $\delta^{13}C_{SOC}$ in particle size separates from soils of variable texture collected within four narrow climatic regimes of Australia. In general, $\delta^{13}C_{SOC}$ becomes more ^{13}C-enriched with decreasing particle size due to a combination of several factors, a phenomenon that has been demonstrated by a number of similar analyses (Bird and Pousai, 1997; Bird et al., 2001; Wynn et al., 2005). Bird et al. (2002a) further used ^{14}C analyses to show that much of this effect is due to an increase in mean residence time of SOC preserved in association with fine particles, particularly fractions less than 63 μm diameter, in which SOC is preserved as 'particulate' organic matter rather than 'mineral-associated' organic matter, the latter of which may be stabilized in soil aggregates. We have already discussed the role of the terrestrial Suess effect in the context of temperature control on SOC residence time in sandy soils. However, this process is also likely to account for much of the difference we observe between the coarse fractions (most recently assimilated C and finest fraction (most stable and oldest C) of soils from dominantly C_3 vegetation (tropical and temperate forests of

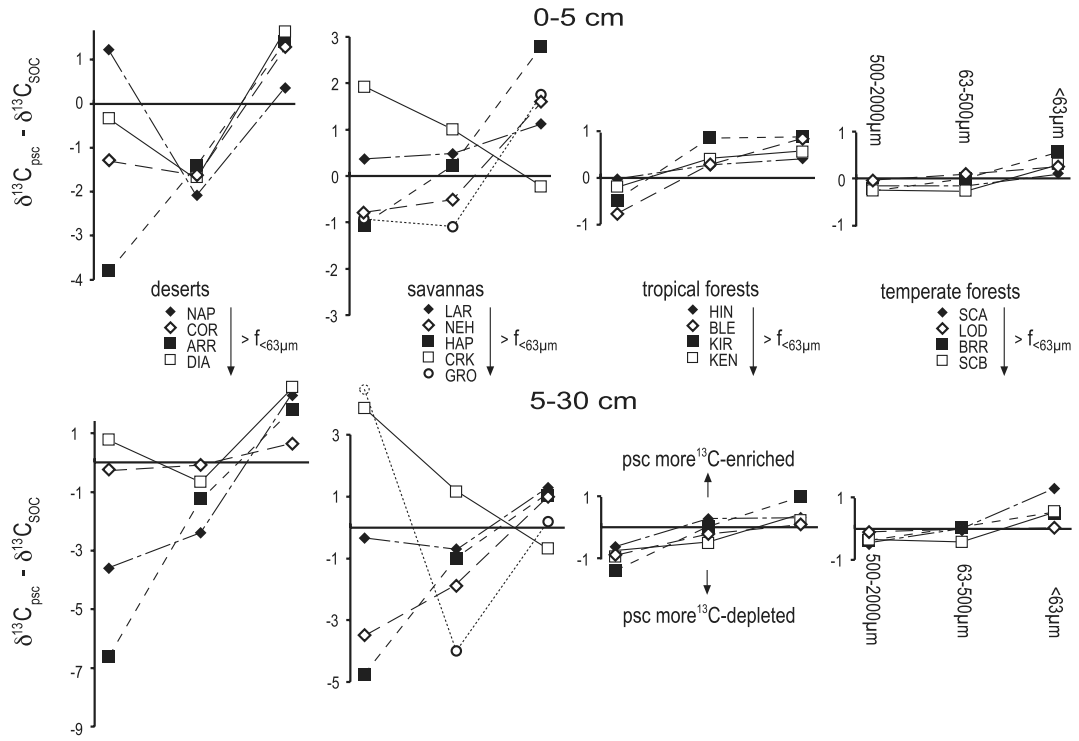

Fig. 9. Difference between carbon isotope ratio of particle size classes ($\delta^{13}C_{psc}$) and bulk soil ($\delta^{13}C_{SOC}$) measured on three physically separated particle size fractions (500–2000 μm, 63–500 μm and <63 μm) for both the 0–5 cm and 5–30 cm intervals of variable texture soil regions sampled from Australia in four climatic zones. Each group of soil regions are sampled from within narrow climatic constraints in four climate zones of Australia (deserts of outback Queensland, semi-arid savannas of central Queensland, tropical forests of coastal north Queensland, and temperate forests of Tasmania; Fig. 1). Within each group, sites are listed in order of increasing fine fraction. Positive values indicate a particle size fraction more ^{13}C-enriched than bulk soil, negative values more ^{13}C-depleted in the particle size.

Fig. 9). In these climates, where vegetation is dominated by C_3 biomass, differences up to 1.6‰ are observed, with the <63 μm fraction consistently more ^{13}C-enriched than coarser fractions. We note that as the relationships between $\delta^{13}C_{SOC}$ and climate were derived only from sandy soils ($f_{<63\,\mu m}$ <0.1), the values for SOC stabilization by fine mineral particles, particularly in the 0–5 cm interval on which the modelled relationships are based, will be low.

In soils of mixed C_3–C_4 vegetation, a number of other factors must account for up to 9‰ differences between coarse and fine particle size separates. In general, similar trends are observed, in that the <63 μm fraction is more ^{13}C-enriched than bulk soil, and the >63 μm fractions are more ^{13}C-depleted (with several exceptions). These data suggest that SOC enriched in ^{13}C by several per mil is preferentially preserved by interaction with fine mineral particles. However, because this variation is outside the range of isotopic disequilibrium values for the terrestrial Suess effect, we must consider several additional possibilities: (1) increased input from C_3 biomass during the time frame of the mean residence time of the 0–5 cm SOC pool (either due to natural or anthropogenic causes), (2) selective input of C_3 biomass to coarse fractions and C_4 biomass to fine fractions or (3) selective preservation of C_4-derived SOC over C_3-derived SOC in the fine fractions of soil. Because our sampling avoided areas of anthropogenic disturbance of the 'natural' C_3–C_4 ratio (minimizing the effects of 1), (2) has not been observed to our knowledge. We consider these trends to record a general increase in the productivity of C_3 biomass in these mixed C_3/C_4 ecosystems due to natural CO_2-fertilization of C_3 plants, a factor predicted by theoretical constraints (Farquhar, 1997).

4. Conclusions

This study has attempted to account for the factors controlling the carbon isotopic composition of the surface pool of SOC at the scale of the Australian continent by using a uniformly collected and analysed data set covering the natural variation of climatic, edaphic and biotic controls at that scale. Our analysis of the climatic effects on $\delta^{13}C_{SOC}$ examines a sample set of sandy soils, which limits variation of edaphic factors controlling decomposition rates and stabilization of SOC by fine mineral particles. Using this data set, our multivariate statistical analyses suggest that the annual availability of water in an ecosystem (W) is the primary control on soil carbon isotope values in Australia's

deserts and savannas, primarily through control of the ratio of C_3–C_4 productivity, and their contribution to SOC. We model the natural variation of $\delta^{13}C_{SOC}$ in sandy soils with a simple function describing the optimized competition between C_3 and C_4 plants, which have variable water use efficiency. Our model emphasizes the water-use advantage of C_4 plants over C_3 plants in environments where water availability is a limiting factor for plant physiological processes—conditions that predominate in Australia. Building on this model of optimized water-use efficiency, we also use temperature effects on soil organic matter decomposition rates, and the resultant effect of variation in the mean residence time of soil organic carbon, on the degree to which the terrestrial Suess effect is incorporated into the bulk SOC pool.

Model regression of our data collected from wide ranging environments across Australia, and including sampled regions outside the Australian climatic variation, accounts for 92% of the variance of $\delta^{13}C_{SOC}$ observed. None of the sandy soil regions in Australia shows a $\delta^{13}C_{SOC}$ value typical of SOC derived entirely from C_4 biomass, which we suggest indicates the selective preservation in the SOC pool of C_3-derived biomass over C_4-derived biomass.

Edaphic controls on the carbon isotopic composition of SOC are considered using similarly collected data on particle size separates from soils of variable texture collected within narrow climatic constraints. Our data for C_3-dominated environments are consistent with the protection of a ^{13}C-enriched pool of old, stable SOC in association with fine mineral particles, and relatively ^{13}C-depleted particulate SOC from fresh biomass, with a magnitude of the difference between fine and coarse fractions consistent with the terrestrial Suess effect. Particle size separate data from mixed C_3–C_4 environments are consistent with natural CO_2-fertilization of C_3 biomass by rising atmospheric CO_2, and the resultant increase in the competitive advantage of C_3 vegetation.

Because accurate C cycle predictions rely on the ability of models to represent fundamental controlling processes, and on validation by comprehensive data sets collected over a wide range of controlling environmental conditions, we propose that enhanced model representation of isotopic processes in the soil organic carbon pool will: (1) provide more rigorous constraints on global CO_2 flux magnitudes from terrestrial systems, (2) identify and quantify sources of CO_2 flux to the atmosphere and (3) quantify the residence times of C fixed from atmospheric CO_2 in biomass and SOC in larger-scale C cycle models (Ciais et al., 1995; Fung et al., 1997; Bakwin et al., 1998; Battle et al., 2000). Additional benefits of the fusion of this model with SOC isotope data collected over expansive environmental gradients (such as latitudinal, precipitation, temperature transects) include: (1), tools for the validation of global models of the ^{13}C discrimination during CO_2 assimilation by the terrestrial biosphere (Lloyd and Farquhar, 1994; Still et al., 2003; Suits et al., 2005), (2) further understanding of the role of pedogenic processes on spatial trends of carbon, nitrogen and sulphur isotopes, all of which typically show enrichment of the heavy isotope with depth and with organic matter quality or 'age' (Novák et al., 2003; Wynn et al., 2005), (3) providing baselines for interpretations of past vegetation change, which are based on changes of carbon isotope composition with depth in soils (Skjemstad et al., 1990; Bonde et al., 1992; Boutton, 1996; Roscoe et al., 2001) and (4) fundamental constraints for much palaeoclimatic research that is underpinned by an understanding of the stable isotopic composition of SOC and soil-respired CO_2, such as constraints on C cycle through geological time (Bird et al., 1994), palaeo-CO_2 barometry (Cerling, 1992b; Bowen and Beerling, 2004) and palaeoclimatic, palaeovegetation and palaeodietary history from fossil materials such as palaeosol organic matter and carbonate, phytoliths, tooth enamel, bone collagen and guano deposits (cf. Cerling, 1984; Cerling et al., 1989; Cerling and Quade, 1993; Koch et al., 1994; Kelly et al., 1998; Koch, 1998).

5. Acknowledgments

We thank the Australian Cooperative Research Centre for Greenhouse Accounting for funding this research. The field assistance of Lins Vellen, Youping Zhou, Delphine Derrien, Joe Cali and Emilie Grand-Clement greatly facilitated the collection of the nearly 1.2 km of soil core collected for this work. Analytical work was accomplished in the stable isotope laboratories of the Earth Environment research group of the Research School of Earth Sciences, the Australian National University, with the technical help of Joan Cowley, Joe Cali, and Lins Vellen and in the FEEA Stable Isotope Laboratory at the University of St. Andrews, Scotland. At least four anonymous reviewers have contributed valuable comments and suggestions to versions of this manuscript.

References

Ågren, G. J., Bosatta, E. and Balesdent, J. 1996. Isotope discrimination during decomposition of organic carbon: a theoretical analysis. *Soil Sci. Soc. Am. J.* **60**, 1121–1126.

Amelung, W., Flach, K.-W. and Zech, W. 1999. Lignin in particle-size fractions of native grassland soils as influence by climate. *Soil Sci. Soc. Am. J.* **63**, 1222–1228.

Bakwin, P. S., P. P., T. and White, J. W. C. 1998. Determination of the isotopic ($^{13}C/^{12}C$) discrimination by terrestrial biology from a global network of observations. *Global Biogeochem. Cycles* **12**, 555–562.

Battle, M., Bender, M. L. and Tans, P. P. 2000. Global carbon sinks and their variability inferred from atmospheric O_2 and $\delta^{13}C$. *Science* **287**, 2467–2470.

Battle, M., Bender, M. L., Tans, P. P., White, J. W. C., Ellis, J. T., and co-authors. 2000. Global carbon sinks and their variability inferred from atmospheric O_2 and $\delta^{13}C$. *Science* **287**, 2467–2470.

Berg, B., Berg, M. P., Bottner, P., Box, E., Breymeyer, A., and co-authors. 1993. Litter mass loss rates in pine forests of Europe and Eastern United States: some relationships with climate and litter quality. *Biogeochemistry* **20**, 127–159.

Berry, S. L. and Roderick, M. L. 2002a. Estimating mixtures of leaf functional types using continental-scale satellite and climatic data. *Global Ecol. Biogeogr.* **11**, 23–39.

Berry, S. L. and Roderick, M. L. 2002b. CO_2 and land-use effects on Australian vegetation over the last two centuries. *Aust. J. Bot.* **50**, 511–531.

Berry, S. L. and Roderick, M. L. 2004. Gross primary productivity and transpiration flux of the Australian vegetation from 1788 to 1988 AD: effects of CO_2 and land use change. *Global Change Biol.* **10**, 1884–1898.

Bird, M. I. and Pousai, P. 1997. Variations of $\delta^{13}C$ in the surface soil organic carbon pool. *Global Biogeochem. Cycles* **11**, 313–322.

Bird, M. I., Haberle, S. G. and Chivas, A. R. 1994. Effect of altitude on the carbon-isotope composition of forest and grassland soils from Papua New Guinea. *Global Biogeochem. Cycles* **8**, 13–22.

Bird, M. I., Chivas, A. R. and Head, J. 1996. A latitudinal gradient in carbon turnover times in forest soils. *Nature* **381**, 143–146.

Bird, M., Šantrůčková, H., Lloyd, J. and Veenendaal, E. 2001. Global soil organic carbon pool. In: *Global Biogeochem. Cycles in the Climate System* (eds E.-D. Schulze, M. Heimann, S. Harrison, E. Holland and J. Lloyd). London Academic Press, 185–199.

Bird, M., Šantrůčková, H., Lloyd, J. and Lawson, E. 2002a. The isotopic composition of soil organic carbon on a north-south transect in western Canada. *Eur. J. Soil Sci.* **53**, 393–403.

Bird, M. I., Šantrůčková, H., Arneth, A., Lloyd, J. J., Gleixner, G., and co-authors. 2002b. Inventories of carbon and isotopes on a latitude gradient through central Siberia. *Tellus* **54B**, 631–641.

Bird, M. I., Veenendaal, E. M. and Lloyd, J. J. 2003. Soil carbon inventories and $\delta^{13}C$ along a moisture gradient in Botswana. *Global Change Biol.* **9**, 1–8.

Bolin, B. and Keeling, C. D. 1963. Large-scale atmospheric mixing as deduced from the seasonal and meridional variations of carbon dioxide. *J. Geophys. Res.* **68**, 3899–3920.

Bonde, T. A., Christensen, B. T. and Cerri, C. C. 1992. Dynamics of soil organic matter as reflected by natural ^{13}C abundance in particle size fractions of forested and cultivated oxisols. *Soil Biol. Biochem.* **24**, 275–277.

Boutton, T. W. 1996. Stable carbon isotope ratios of soil organic matter and their use as indicators of vegetation and climate change. In: *Mass Spectrometry of Soils* (eds T. W. Boutton and S. I. Yamasaki). Marcel-Dekker, New York, 47–81.

Bowen, G. J. and Beerling, D. J. 2004. An integrated model for soil organic carbon and CO_2: implications for paleosol carbonate pCO_2 paleobarometry. *Global Biogeochem. Cycles* **18**, GB1026.

Brady, N. C. and Weil, R. R. 2002. *The Nature and Properties of Soils*. Prentice Hall, Upper Saddle River, NJ.

Brugnoli, E. and Farquhar, G. D. 2000. Photosynthetic fractionation of carbon isotopes. In: *Photosynthesis: Physiology and Metabolism* (eds R. C. Leegood, T. D. Sharkey and S. von Caemmerer). Kluwer, Dordrecht, 399–434.

Brugnoli, E., Hubick, K. T., von Caemmerer, S. and Farquhar, G. D. 1988. Correlation between the carbon isotope discrimination in leaf starch and sugars of C_3 plants and the ratio of intercellular and atmospheric partial pressures of carbon dioxide. *Plant Physiol.* **88**, 1418–1424.

Buchmann, N., Brooks, J. R., Rapp, K. D. and Ehleringer, J. R. 1996. Carbon isotope composition of C_4 grasses is influenced by light and water supply. *Plant Cell Environ.* **19**, 392–402.

Cerling, T. E. 1984. The stable isotopic composition of soil carbonate and its relationship to climate. *Earth Planet. Sci. Lett.* **71**, 229–240.

Cerling, T. E. 1992a. Development of grasslands and savannas in East Africa during the Neogene. *Palaeogeogr. Palaeoclimatol. Palaeoecol.* **97**, 241–247.

Cerling, T. E. 1992b. Use of carbon isotopes in paleosols as an indicator of the $p(CO_2)$ of the paleoatmosphere. *Global Biogeochem. Cycles* **6**, 307–314.

Cerling, T. E. and Quade, J. 1993. Stable carbon and oxygen isotopes in soil carbonates. In: *Climate Change in Continental Isotope Records* (eds P. K. Swart, K. C. Lohmann, J. A. McKenzie and S. Savin), 217–231.

Cerling, T. E., Quade, J., Wang, Y. and Bowman, J. R. 1989. Carbon isotopes in soils and palaeosols as ecology and paleoecology indicators. *Nature* **341**, 138–139.

Cerling, T. E., Harris, J. M., MacFadden, B. J., Leakey, M. G., Quade, J., and co-authors. 1997. Global change through the Miocene/Pliocene boundary. *Nature* **389**, 153–158.

Cerling, T. E., Ehleringer, J. R. and Harris, J. M. 1998. Carbon dioxide starvation, the development of C_4 ecosystems, and mammalian evolution. *Philos. Trans. Roy. Soc., Lond. B* **353**, 159–171.

Cerling, T. E., Harris, J. M. and Passey, B. H. 2003. Diets of East African bovidae based on stable isotope analysis. *J. Mammal.* **84**, 456–470.

Chapin, F. S., Matson, P. A. and Mooney, H. A. 2002. *Principles of Terrestrial Ecosystem Ecology*. Springer, New York.

Chelle, M. 2005. Phylloclimate or the climate perceived by individual plant organs: what is it? How to model it? What for? *New Phytologist* **166**, 781–790.

Ciais, P., Tans, P. P., White, J. W. C., Trolier, M., Francey, R. J., and co-authors. 1995. Partitioning of ocean and land uptake of CO_2 as inferred by $\delta^{13}C$ measurements from the NOAA Climate Monitoring and Diagnostic Laboratory Global Air Sampling Network. *J. Geophys. Res.* **100**, 5051–5070.

Ciais, P., Cuntz, M., Scholze, M., Mouillot, F., Peylin, P., and co-authors. 2005. Remarks on the use of ^{13}C and ^{18}O isotopes to quantify biospheric carbon fluxes. In: *Stable Isotopes and Biosphere-Atmosphere Interactions* (eds L. B. Flanagan, J. R. Ehleringer and D. E. Pataki). Elsevier, Amsterdam, 235–267.

Ciais, P., Tans, P. P., White, J. W. C., Trolier, M., Francey, R. J., and co-authors. 1995. Partitioning of ocean and land uptake of CO_2 as inferred by $\delta^{13}C$ measurements from the NOAA climate monitoring and diagnostic laboratory global air sampling network. *J. Geophys. Res.* **100**, 5051–5070.

Collatz, G. J., Berry, J. A. and Clark, J. S. 1998. Effects of climate and atmospheric CO_2 partial pressure on the global distribution of C_4 grasses: present, past, and future. *Oecologia* **114**, 441–454.

Comstock, J. P. and Ehleringer, J. R. 1992. Correlating genetic variation in carbon isotopic composition with complex climatic gradients. *Proc. Natl. Acad. Sci.* **89**, 7747–7751.

Cowan, I. R. 1977. Stomatal behaviour and environment. *Adv. Botanical Res.* **4**, 471–505.

Cowan, I. R. and Farquhar, G. D. 1977. Stomatal function in relation to leaf metabolism and environment. *Symp. Soc. Exp. Biol.* **31**, 471–505.

Deines, P. 1980. The isotopic composition of reduced organic carbon. In: *Handbook of Environmental Isotope Geochemistry. I. The Terrestrial Environment* (eds P. Fritz and J. C. Fontes). Elsevier, Amsterdam, 329–406.

DeLucia, E. H. and Schlesinger, W. H. 1991. Resource-use efficiency and drought tolerance in adjacent Great Basin and Sierran plants. *Ecology* **72**, 51–58.

Ehleringer, J. R. 1993. Carbon and water relations in desert plants: an isotopic perspective. In: *Stable Isotopes and Plant Carbon-Water Relations* (eds J. R. Ehleringer, A. E. Hall and G. D. Farquhar). Academic Press, New York.

Ehleringer, J. R. and Björkman, O. 1977. Quantum yields for CO_2 uptake in C_3 and C_4 plants: dependence on temperature, CO_2 and O_2 concentrations. *Plant Physiol.* **59**, 86–90.

Ehleringer, J. R., Field, C. B., Line, Z.-F. and Kuo, C.-Y. 1986. Leaf carbon isotope and mineral composition in subtropical plants along an irradiance cline. *Oecologia* **70**, 520–526.

Ehleringer, J. R., Sage, R. F., Flanagan, L. B. and Pearcy, R. W. 1991. Climate change and the evolution of C_4 photosynthesis. *Trends Ecol. Evol.* **6**, 95–99.

Ehleringer, J. R., Cerling, T. E. and Helliker, B. R. 1997. C_4 photosynthesis, atmospheric CO_2, and climate. *Oecologia* **112**, 285–299.

Ehleringer, J. R., Hall, A. E. and Farquhar, G. D. 1993. *Stable Isotopes and Plant Carbon-Water Relations*. New York, Academic.

Farquhar, G. D. 1997. Carbon dioxide and vegetation. *Science* **278**, 1411.

Farquhar, G. D. and Richards, R. A. 1984. Isotopic composition of plant carbon correlates with water-use efficiency of wheat genotypes. *Aust. J. Plant Physiol.* **11**, 539–552.

Farquhar, G. D., von Caemmerer, S. and Berry, J. A. 1980. A biochemical model of photosynthetic CO_2 assimilation in leaves of C_3 species. *Planta* **149**, 78–90.

Farquhar, G. D., O'Leary, M. H. and Berry, J. A. 1982a. On the relationship between carbon isotope discrimination and the intercellular carbon dioxide concentration in leaves. *Aust. J. Plant Physiol.* **9**, 121–127.

Farquhar, G. D., Ball, M. C., von Caemmerer, S. and Roksandic, Z. 1982b. Effects of salinity and humidity on $\delta^{13}C$ values of halophytes—evidence for diffusional isotope fractionation determined by the ratio of intercellular/atmospheric partial pressure of CO_2 under different environmental conditions. *Oecologia* **52**, 121–124.

Farquhar, G. D., Hubick, K. T., Condon, A. G. and Richards, R. A. 1988. Carbon isotope fractionation and plant water-use efficiency. *Ecol. Stud.* **68**, 21–40.

Farquhar, G. D., Ehleringer, J. R. and Hubick, K. T. 1989. Carbon isotope discrimination and photosynthesis. *Ann. Rev. Plant Physiol. Plant Mole. Biol.* **40**, 503–537.

Flanagan, L. B., Ehleringer, J. R. and Pataki, D. E. 2005. *Stable Isotopes and Biosphere-Atmosphere Interactions*. Amsterdam, Elsevier.

Francey, R. J., Tans, P. P., Allison, C., Enting, I. G. and White, J. W. C. 1995. Changes in oceanic and terrestrial carbon uptake since 1982. *Nature* **373**, 326–330.

Fung, I., Field, C. B., Berry, J. A., Thompson, M. V., Randerson, J. T., and co-authors. 1997. Carbon-13 exchanges between the atmosphere and biosphere. *Global Biogeochem. Cycles* **11**, 507–533.

Gates, D. M. 1968. Transpiration and leaf temperature. *Ann. Rev. Plant Physiol.* **19**, 211–238.

Grace, J., Lloyd, J., Miranda, A. C., Miranda, H. and Gash, J. H. C. 1998. Fluxes of carbon dioxide and water vapor over a C_4 pasture in south-western Amazonia (Brazil). *Aust. J. Plant Physiol.* **25**, 519–530.

Hatch, M. D. 1987. C_4 photosynthesis: a unique blend of modifed biochemistry, anatomy and ultrastructure. *Biochem. Biophys. Acta* **895**, 81–106.

Kätterer, T., Reichstein, M. and Andren, O. 1998. Temperature dependence of organic matter decomposition: a critical review using literature data analyzed with different models. *Biol. Fertility Soils* **27**, 258–262.

Keeling, C. D., Bacastow, R. B., Carter, A. F., Piper, S. C., Whorf, T. P., and co-authors. 1989. A three dimensional analysis of atmospheric CO_2 transport based on observed winds (4) Mean annual gradients and interannual variations. In: *Aspects of Climate Variability in the Pacific and Western Americas* (ed D. H. Peterson). AGU, Washington, DC, 305–363.

Kelly, E. F., Blecker, S. W., Yonker, C. M., Olson, C. G., Wohl, E. E., and authors. 1998. Stable isotope composition of soil organic matter and phytoliths as paleoenvironmental indicators. *Geoderma* **82**, 59–81.

Kirschbaum, M. U. F. 1995. The temperature dependence of soil organic matter decomposition and the effect of global warming on soil organic carbon storage. *Soil Biol. Biochem.* **27**, 753–760.

Koch, P. L. 1998. Isotopic reconstruction of past continental environments. *Ann. Rev. Earth Planet. Sci.* **26**, 573–613.

Koch, P. L., Fogel, M. L. and Tuross, N. 1994. Tracing the diets of fossil animals using stable isotopes. In: *Methods in Ecology* (eds K. Lajtha and B. Michener). Blackwell Scientific Press, Oxford, 63–92.

Lenton, T. M. and Huntingford, C. 2003. Global terrestrial carbon storage and uncertainties in its temperature sensitivity examined with a simple model. *Global Change Biol.* **9**, 1333–1352.

Levin, N. L., Quade, J., Simpson, S. W., Semaw, S. and Rogers, M. 2004. Isotopic evidence for Plio-Pleistocene environmental change at Gona, Ethiopia. *Earth Planet. Sci. Lett.* **219**, 93–110.

Liski, J., Nissinen, A. and Erhard, M. 2003. Climatic effects on litter decomposition from artic tundra to tropical rainforest. *Global Change Biol.* **9**, 575–584.

Lloyd, J. and Farquhar, G. D. 1994. ^{13}C discrimination during CO_2 assimilation by the terrestrial biosphere. *Oecologia* **99**, 201–215.

Lloyd, J. and Taylor, J. A. 1994. On the temperature dependence of soil respiration. *Funct. Ecol.* **8**, 315–323.

Long, S. P. 1999. Environmental Responses. In: *C_4 Plant Biology* (eds R. F. Sage and R. K. Monson). Academic, San Diego, 215–249.

Marshall, J. D. and Zhang, J. 1994. Carbon isotope discrimination and water-use efficiency in native plants of the north-central Rockies. *Ecology* **75**, 1887–1895.

Meentemeyer, V. 1978. An approach to the biometeorology of decomposer organisms. *Int. J. Biometeorol.* **22**, 94–102.

Nobel, P. S. 1994. *Remarkable Agaves and Cacti*. New York, Oxford University Press.

Nobel, P. S. 2005. *Plant Physiology*. Amsterdam, Elsevier.

Novák, M., Buzek, F., Harrison, A. F., Prechová, E., Jacková, I., and co-authors. 2003. Similarity between C, N and S stable isotope profiles in European spruce forest soils: implications for the use of $\delta^{34}S$ as a tracer. *Appl. Geochem.* **18**, 765–779.

O'Leary, M. H. 1981. Carbon isotope fractionation in plants. *Phytochemistry* **20**, 553–567.

Oke, T. R. 1992. *Boundary Layer Climates*. London, Routledge.

Osmond, C. B., Winter, K. and Ziegler, H. 1982. Functional significance of different pathways of CO_2 fixation in photosynthesis. In: *Physiological Plant Ecology: Water Relations and Carbon*

Assimilation (eds O. L. Lange, P. S. Nobel, C. B. Osmond and H. Ziegler). Springer-Verlag, Berlin, 480–547.

Quade, J. and Cerling, T. E. 1995. Expansion of C_4 grasses in the Late Miocene of Northern Pakistan: evidence from stable isotopes in paleosols. *Palaeogeogr. Palaeoclimatol. Palaeoecol.* **115**, 91–116.

Randerson, J. T., Collatz, G. J., Fessenden, J. E., Munoz, A. D., Still, C. J., and co-authors. 2002. A possible global covariance between terrestrial gross primary production and ^{13}C discrimination: consequences for the atmospheric ^{13}C budget and its response to ENSO. *Global Biogeochem. Cycles* **16**, 1136.

Roscoe, R., Buurman, P., Velthorst, E. J. and Vasconcellos, C. A. 2001. Soil Organic Matter dynamics in density and particle size fractions as revealed by the $^{13}C/^{12}C$ isotopic ratio in a Cerrado's oxisol. *Geoderma* **104**, 185–202.

Sage, R. F. 2004. The evolution of C_4 photosynthesis. *New Phytologist* **161**, 341–370.

Sage, R. F. and Pearcy, R. W. 1987. The nitrogen use efficiency of C_3 and C_4 plants. *Plant Physiol.* **84**, 959–963.

Sanderman, J., Amundson, R. G. and Baldocchi, D. D. 2003. Application of eddy covariance measurements to the temperature dependence of soil organic matter mean residence time. *Global Biogeochem. Cycles* **17**, 1061–1075.

Sandquist, D. R. and Ehleringer, J. R. 1995. Carbon isotope discrimination in the C_4 shrub Atriplex confertifolia (Torr. & Frem.) Wats. along a salinity gradient. *Great Basin Naturalist* **55**, 135–141.

Šantrůčková, H., Bird, M. I. and Lloyd, J. 2000. Microbial processes and carbon-isotope fractionation in tropical and temperate grassland soils. *Funct. Ecol.* **14**, 108–114.

Schleser, G. H., Frielingsdorf, J. and Blair, A. 1999. Carbon isotope behaviour in wood & cellulose during artificial aging. *Chem. Geol.* **158**, 121–130.

Schulze, E.-D. and Hall, A. E. 1982. Stomatal responses, water loss and CO_2 assimilation rates of plants in contrasting environments. In: *Physiological Plant Ecology: Water Relations and Carbon Assimilation* (eds O. L. Lange, P. S. Nobel, C. B. Osmond and H. Ziegler). Springer-Verlag, Berlin, 181–230.

Skjemstad, J. O., Le Feuvre, R. P. and Prebble, R. E. 1990. Turnover of soil organic matter under pasture as determined by ^{13}C natural abundance. *Aust. J. Soil Res.* **28**, 267–276.

Still, C. J., Berry, J. A., Collatz, J. G. and DeFries, R. S. 2003. Global distribution of C_3 and C_4 vegetation: carbon cycle implications. *Global Biogeochem. Cycles* **17**, 1006.

Stuiver, M. and Braziunas, T. F. 1987. Tree cellulose $^{13}C/^{12}C$ isotope ratios and climate change. *Nature* **328**, 58–60.

Suits, N., Denning, A. S., Berry, J. A., Still, C. J., Miller, J. B., and co-authors. 2005. Simulation of carbon isotope discrimination of the terrestrial biosphere. *Global Biogeochem. Cycles* **19**, 1017.

Teeri, J. A. 1988. Interaction of temperature and other environmental variables influencing plant distribution. In: *Plants and Temperature* (eds S. P. Long and F. I. Woodward). Company of Biologists, Ltd., Cambridge, 77–89.

Trumbore, S. E. 1997. Potential responses of soil organic carbon to global environmental change. *Proc. Natl. Acad. Sci.* **94**, 8284–8291.

Trumbore, S. E. 2000a. Age of soil organic matter and soil respiration: radiocarbon constraints on belowground C dynamics. *Ecol. Appl.* **10**, 399–411.

Trumbore, S. E. 2000b. Constraints on below-ground carbon cycling from radiocarbon: the age of soil organic matter and respired CO_2. *Ecol. Appl.* **10**, 399–411.

Van Der Merwe, N. J. and Medina, E. 1989. Photo-synthesis & $^{13}C/^{12}C$ ratios in Amazonian rain forests. *Geochim. Cosmochim. Acta* **53**, 1091–1094.

Vogel, J. C. 1978. Recycling of carbon in a forest environment. *Oecologia Plantarum* **13**, 89–94.

Winter, K., Holtum, J. A. M., Edwards, G. E. and O'Leary, M. H. 1982. Effect of low relative humidity on $\delta^{13}C$ values in two C_3 grasses and ain Panicum milloides, a C_3-C_4 intermediate species. *J. Exp. Bot.* **33**, 88–91.

Wynn, J. G. 2004. Influence of Plio-Pleistocene aridification on human evolution: evidence from paleosols of the Turkana Basin, Kenya. *Am. J. Phys. Anthropol.* **123**, 106–118.

Wynn, J.G. and Bird, M.I. 2007. C_4-derived soil organic carbon decomposes faster than its C_3 counterpart. *Global Change Biol.* **13**, 2206–2217.

Wynn, J. G., Bird, M. I. and Wong, V. N. L. 2005. Rayleigh distillation and the depth profile of $^{13}C/^{12}C$ ratios in soil organic carbon from two soils in Iron Range National Park, Far North Queensland, Australia. *Geochim. Cosmochim. Acta* **69**, 1961–1973.

Wynn, J. G., Bird, M. I., Vellen, L., Grand-Clement, E., and co-authors. 2006. Continental-scale measurement of the soil organic carbon pool with climatic, edaphic, and biotic controls. *Global Biogeochem. Cycles* **20**, GB1007, doi:1010.1029/2005GB002576.